DOCTORAL THESIS

Automation of Front-End Loaders

Electronic Self Leveling and Payload Estimation

I YUNG

Robotics and Control Group
Department of Applied Physics and Electronics
UMEÅ UNIVERSITY, SWEDEN
Umeå, 2017

Department of Applied Physics and Electronics
Umeå University, Sweden
SE-90187 UMEÅ
Author e-mail: iyung.ong@umu.se

Thesis submitted for the degree of Doctor of Philosophy (Ph.D.)
in Applied Physics and Electronics with specialization in Control Engineering.

Akademisk avhandling för avläggande av teknologie doktorsexamen (Tekn. Dr.)
i Tillämpad elektronik med inriktning mot reglerteknik.

ISSN 1654-5419:8
ISBN 978-91-7601-709-8
E-version available at http://umu.diva-portal.org
Printed by Print & Media, Umeå University, Umeå, May 2017

Automation of Front-End Loaders

Electronic Self Leveling and Payload Estimation

I Yung

Robotics and Control Group, Umeå University, Sweden

ABSTRACT

A growing population is driving automatization in agricultural industry to strive for more productive arable land. Being part of this process, this work is aimed to investigate the possibility to implement sensor-based automation in a particular system called Front-End Loader, which is a lifting arm that is commonly mounted at the front of a tractor. Two main tasks are considered here, namely Electronic Self Leveling (ESL) and payload estimation. To propose commercially implementable solutions for these tasks, specific objectives are set, which are: 1) to propose a controller to perform ESL under typical disturbances 2) to propose a methodology for payload estimation considering realistic estimation conditions. Lastly, aligned with these goals, 3) to propose models for the Front End Loader under consideration for derivation of solutions of the specified tasks.

The self-leveling task assists farmers in maintaining the angular position of the mounted implement, e.g. a bale handler or a bucket, with respect to the ground when the loader is manually lifted or lowered. Experimental results show that different controllers are required in lifting and lowering motions to maintain the implement's angular position with a required accuracy due to principle differences in gravity impact. The gravity helps the necessary correction in lifting motion, but works against the correction in lowering motions. This led us to propose a controller with a proportional term, a discontinuous term and an on-line disturbance estimation and compensation as well as the tuning procedure to achieve a 2 degrees tracking error for lowering motions in steady state. The proposed controller shows a less sensitive performance to lowering velocity, as the main disturbance, in comparison to a linear controller.

The second task, payload estimation, assists farmers to work within safety range as well as to work with a weight measurement tool. A mechanical model, derived based on equations of motion, is improved by a pressure based friction to sufficiently accurately represent the motion of the front end loader under consideration. The proposed model satisfies the desired estimation accuracy of 2% full scale error in a certain estimation condition domain in constant velocity regions, with off-line calibration step and off-line payload estimation step. An on-line version of the estimation, based on Recursive Least Squares, also fulfills the desired accuracy, while keeping the calibration step off-line.

Automatisering av frontlastare

Elektrisk parallellföring och vägningsfunktion

I Yung

Robotik och reglerteknik, Umeå universitet, Sverige

SAMMANFATTNING

En växande befolkning driver fram automatisering inom jordbruksindustrin genom en strävan efter mer produktiv åkermark. Som delaktig i denna process, syftar detta arbete till att undersöka möjligheten att implementera sensorbaserad automatisering på ett särskilt typ av system kallad frontlastare, som är en hydraulisk lyftanordning som vanligen monteras framtill på en jordbrukstraktor. Två huvudfunktioner undersöks här, nämligen en funktion för elektrisk parallellföring av redskap och en funktion för uppskattning av nyttolast. För att realisera kommersiella lösningar till dessa funktioner, har vi specificerat följande mål: 1) föreslå en regulator för att realisera elektrisk parallellföring under typiska störningsförhållanden, 2) föreslå en algoritm för lastvägning under realistiska driftsförhållanden. Slutligen, i linje med dessa mål, 3) föreslå modeller för den aktuella frontlastaren för härledning av lösningar till de önskade funktionerna.

Parallellföringsfunktionen hjälper jordbrukare att bibehålla en önskad vinkel på det påmonterade redskapset, t.ex. en balgrip eller en skopa, relativt markplanet när redskapet höjs eller sänks. Experimentella resultat visar att olika regulatorer krävs för höj- och sänkrörelser för att bibehålla redskapet vinkelnoggrannet, detta på grund av gravitationens inverkan. Gravitationen bidrar till nödvändig felkorrigering under lyftrörelse, men motverkar nödvändig felkorrigering under sänkrörelse. Detta fick oss att föreslå en regulator bestående av en proportionell del, en diskontinuerlig del, och direkt störningsuppskattning och störningskompensering, samt en kalibreringsmetod för att uppnå max 2 graders vinkelfel under stationär sänkrörelse. Den föreslagna regulatorn är mindre känslig för sänkhastighet, den huvudsakliga störningen, jämfört med en linjär regulator.

Den andra funktionen, uppskattning av nyttolast, kan hjälpa jordbrukare att använda frontlastaren på ett säkert inom dess tillämpningsområde, såväl som att arbeta med viktmätning. En mekanisk modell, härledd baserad på rörelseekvationer, har förbättrats genom tryckbaserad friktion för att tillräckligt noggrant beskriva rörelsen hos den aktuella frontlastaren. Den föreslagna modellen uppfyller den önskade noggrannheten på max 2% fullskaligt fel i en viss estimerings-villkors-domän i konstanta hastighetsområden, detta genom off-line kalibrering och off-line uppskattning av nyttolast. En online version av estimeringen baserat på Rekursiva minsta-kvadrat metoden uppfyller också den önskade noggrannheten, samtidigt som kalibreringen utförs off-line.

List of Publications

Part of the works presented in this thesis have passed peer-reviewed conferences. Four of the publications, including two manuscripts, are reproduced in the second part of this thesis, and will be referred to by alphabetical orders:

(A) I Yung, C. Vázquez, and L. Freidovich. Automation of front-end loaders: self leveling task. In *Proceedings of the 20th IEEE Conference on Emerging Technologies Factory Automation (ETFA)*. pp. 1-7. Luxembourg, Sept. 2015.

(B) I Yung, C. Vázquez, and L. Freidovich. Control and Tuning Procedure of a Cylinder in Mobile Hydraulics. 2016. Submitted manuscript.

(C) I Yung, C. Vázquez, and L. Freidovich. Payload estimation in front-end loaders. In *Proceedings of the 5th International Conference on Machine Control & Guidance (MCG)*. Vichy, Oct. 2016.

(D) I Yung, L. Freidovich, C. Vázquez, and S. Rönnbäck. Improvement of Model-Based Payload Estimation for Agricultural Front-End Loaders. 2017. Submitted manuscript.

The following additional publications, which have also passed peer review process, are not included in the thesis for the consistency of the presentation:

- I Yung, S. Aranovskiy, and L. Freidovich. Case Study on Non-Ideal Current Tracking in Amplifiers for Voltage-Driven Manipulators. In *Proceedings of the 14th Mechatronics Forum International Conference*. Karlstad, June 2014.
- I Yung, L. Freidovich, and T. Nygren. Automation of Front End Loaders Case Study: Self Leveling. Extended abstract in *Swedish Control Conference (Reglermöte)*. Linköping, June 2014.

For all the related papers, I Yung, as the first author, was the main contributor, in particular:

- preparing the first, intermediate, and final drafts of the papers/manuscripts (in paper A-D),
- building and running the simulation models (in paper A-B),
- preparing the hardware, including installation and calibration of additional sensors to the system, checking sensors and valve configurations (in paper A-B),
- performing experimental studies, including experiment designs and planning to evaluate the proposed solutions and partly preparing the setups for implementations (in paper A-D),
- performing data acquisition, analysis and interpretation of the results (in paper A-D),
- delivering oral presentations at international conferences (20 minutes each) for the accepted conference papers (paper A,C).

The co-authors have mainly contributed with feedback resulted from participation in discussions on the possible directions to solve the problems as well as on the manuscripts and on the results and with some suggestions, except for the following more substantial contributions:

(A) In Paper A: The first author together with Carlos Vázquez were implementing and tuning parameters of the controllers in the experiments.

(B) In Paper B: Carlos Vázquez suggested the use of a vector Lyapunov function and the rest of the tuning was done together with the first author.

(C) -

(D) In Paper D: Sven Rönnbäck suggested the direction of the successful investigation towards pressure based friction for the model improvement.

Acknowledgments

The study reported in this thesis is a significant part of an investigation performed at Ålö AB (http://www.alo.se) with financial support from the Swedish Research Council under the industrial doctoral student project grant 2012-4172 *"Automation of front-end loaders for agricultural tractors"*. The author would also like to thank Ålö AB and The Kempe Foundations for their financial support for attending conferences. The results are reported with permission from the company.

I would also like to express my gratitude to people around me throughout this project:

to my supervisors: Leonid Freidovich, Carlos Vázquez, Sven Rönnbäck and Tomas Nygren, for the opportunity, your guidance, encouragement, challenges, discussions and feedback;

to my colleagues at Ålö AB: David Wiberg, Roger Westpil, Mikael Wiberg and Gustaf Lagunoff and people in control systems for their feedbacks and technical supports; Stefan Klein, Clas-Göran Ingman and Kennet Sandström for their assistance to setting up the experiments; Jakob Forsberg and Peter Lindberg for their assistance with the CAD model; Ylva Karlsson for her assistance with the mechanical drawing; Anette Appelblad, Ann-Sofie Löfvenius, Elisabeth Norén and Cecilia Wiking for making the journey more enjoyable;

to everyone at the Department of Applied Physics and Electronics for their cooperation, understanding and support; my office mate Szabolcs Fodor for your patience and company in a similar journey as well as my PhD fellows Christian Brembilla, Muhammad Sikandar Lal Khan, Shoaib Azizi and Helena Nydahl for your company throughout this study;

to Marie Fransson, Susanne Sarin, and Mona-Lisa Gunnarsson for helping me out with administrative matters;

to my Indonesian friends Roya, Ailiana Santosa and Prof. Nawi Ng, and other Indonesian fellows who have been sharing the experience abroad together;

to Fabio for your invaluable support during these years and my family for their support from afar. Your patience is much appreciated;

above all, to God for the strength and blessings throughout this period.

I Yung

Umeå, Sweden, 2017

Contents

1 Introduction

The need to automatize agricultural machineries is driven by growing population. More urban area is expected and hence arable land will be limited. Decrease in agricultural land is indicated in recent reports, which is around 0.8 % less from 2007 to 2012 in US only [10], and around 0.7 % less from 2010 to 2013 in EU [1]. This causes the need to increase the ratio of food production over arable land, which can lead to mechanization of agricultural processes to achieve higher efficiency and accuracy.

Introducing robotic systems in agriculture is believed to have substantial impacts [5], e.g. increase of efficiency in crops production [6]. Machines are good to be utilized for repetitive tasks and tasks in hard conditions [4]. One example is investigation on autonomous vehicles to automatize harvesting [36] and coordination of multiple autonomous vehicles [13]. Besides, machine vision is investigated in [15] to distinguish weeds from the crops.

In larger scale farming, mechanization has started with a tractor as a basic tool. Besides, for its heavy-duty tasks, several hydraulics actuated equipments are used together with tractors. One of the most common equipment is the lifting arm called Front-End Loader (FEL) [23], see Fig. 1.1. Along with the manual operation that is commonly available, the investigation to automate this heavy duty equipment is the main topic of this thesis.

As a heavy-duty machine, development towards automation is also found in other heavy duty machines such as forestry cranes [31] and earth moving machines, e.g. excavators [42]. Common challenges are encountered, especially from the uncontrolled environment such that a careful consideration is required to select the sensors type and location [5]. A sensorless attempt to realize predefined trajectories by open-loop for cranes is reported in [29, 30]. However, in agricultural applications considered here, a driver is still highly expected to partly or fully control the system. Thus, a semi-automation problem is faced here, instead of an autonomous system [11]. In this work, two tasks are

Fig. 1.1: An example of a Front-End Loader with a mounted bale handler as an implement

investigated: Electronic Self-Leveling (ESL) and payload estimation tasks for Front-End Loaders (FELs). The first task can help farmers in duties that involve maintaining implements angular position, such as buckets, forklifts and bale handlers, regardless the boom motion. The second task can help farmers in monitoring and safer handling. Having several tasks successfully automated can allow farmers to focus on other tasks and hence increases productivity.

1.1 Research Goals and Approach

The main objectives of this research are:

1. A controller to realize Electronic Self Leveling task to achieve a tracking error of less than 2 degrees .

2. A procedure to estimate payload with a desired accuracy below 2% Full Scale (FS) error.

To achieve these goals, the following approach has been followed and partly reported in the attached articles in Part II:

To achieve the first goal, a simplified model has been derived for the FEL under consideration. The equations of motion for the mechanical structure and a simplified model of non-linear dynamics of a hydraulic actuator have been derived.

Based on these derivations, a simplified simulation model is built for evaluating controllers to realize the ESL task. A standard Proportional Integral (PI) controller and the proposed controller with an estimated disturbance compensation are compared in this simulation model and in experiments. This work is presented in Paper A.

From the comparison results, a procedure to tune the proposed controller using a Lyapunov function is investigated to obtain the controller parameters for a desired steady state error. Experiments have been performed to evaluate the tuned controller in steady state with the valve under consideration. A comparison with PI controller has also been carried out and presented in Paper B.

Furthermore, experiments and analysis have been performed to deal with saturation due to flow limitation. A safety function is proposed, designed, and tested in experiments to handle insufficient flow.

To achieve the second goal, a simplified mechanical dynamics of the loader is derived. A number of experiments, with variation in estimation conditions, have been carried out to test the proposed payload estimation procedure. The first proposal, with a calibration of boom Center of Gravity (COG) before the estimation step, results in an estimation accuracy of 5% Full Scale (FS) error, which is presented in Paper C. The second proposal (reported in Paper D), which examines possible model improvements, results in the desired estimation accuracy of 2% FS error.

Note that all the experiments and results have been done with a particular FEL mounted on and supplied through a certain hydraulic valve by a flow supply in a stationary tractor. Moreover, all the proposed algorithms require the presence of cylinder pressures and angular position measurements.

1.2 Thesis Outline

The thesis is divided into two parts. The first part of the thesis summarizes the work during the course of doctoral studies; to provide additional references and more detailed analysis that are not presented as scientific papers in Part II. The chapters are aimed to be self-contained.

1.2.1 Summary of Part I : Thesis Work

Part I of the thesis is organized as follows:

Chapter 2: Notations. In this chapter, the system is visually introduced with all the notations that will be used throughout the thesis (with a few minor exceptions).

Chapter 3: Modeling. In this chapter, a FEL model that is constituted by mechanical and hydraulic parts are presented, specifically, a hydraulic cylinder model for the ESL task and a mechanical model for the payload estimation task. Lastly, a description of one of the hydraulic valves used in experiments and an investigation of a supply pressure model are presented.

Chapter 4: Electronic Self Leveling. In this chapter, a simplified simulation model for comparison of controllers is presented. Moreover, a brief summary of Paper A and B is provided. The proposed algorithm that copes with fault detection and mitigation is also presented. Finally, the background theories that are related to control design are presented.

Chapter 5: Payload Estimation. In this chapter, a brief summary of results in Paper C and D is presented.

Chapter 6: Supportive Works. In this chapter, several hardware related works are presented, which are a comparison of two prototyping platforms (dSpace and xPC Target), replacing the existing indirect connection to dSpace of an IMU sensor to a direct one, and calibration of the available angular position measurements. Moreover, the work on design and comparison of online differentiators is also presented.

Chapter 7: Summary of Contributions. In this chapter, the contributions are summarized.

Chapter 8: Conclusions and Future Work. In this chapter, the conclusions and future work are presented.

1.2.2 Summary of Part II: Publications

The second part of the thesis contains the accepted and/or submitted papers with the following summaries.

Paper A: Automation of Front-End Loaders: Self Leveling Task In this paper, an investigation of controllers to realize Electronic Self Leveling (ESL) task has been done in experiments and simulations.

Paper B: Control and Tuning Procedure of a Cylinder in Mobile Hydraulics In this paper, a tuning procedure to find the parameters of the proposed controller to realize ESL for lowering motion is presented. The performance of the tuned controller in steady state is compared to a tuned PI controller in experiments.

Paper C: Payload Estimation in Front-End Loaders In this paper, the challenges of payload estimation in FELs are presented. An offline estimation procedure is proposed based on a simplified model of mechanical dynamics. To evaluate this procedure, a set of experiments with varying velocities and bucket angles has been carried out. The estimation accuracy lies within 5 % Full Scale (FS) error with the proposed procedure.

Paper D: Improvement of Model-Based Payload Estimation for Agricultural Front-End Loaders In this paper, an improvement to the simplified model of the mechanical dynamics is investigated. Based on this improvement, the accuracy of the offline payload estimation is improved to 2% FS error. Moreover, an online payload estimation algorithm has also been proposed and tested.

Part I

Thesis Work

2 Notations and Abbreviations

The following notations and abbreviations will be used in the thesis:

2.1 Abbreviations

ADRC	Active Disturbance Rejection Controller
CAD	Computer-Aided Design
COG	Center of Gravity
DOF	Degree of Freedom
DZ	Dead-Zone
ESL	Electronic Self Leveling
FEL	Front-End Loader
FFT	Fast Fourier Transform
FS	Full Scale
IMU	Inertial Measurement Unit
OC	Open-Center
PI	Proportional Integral controller
PID	Proportional Integral Derivative controller
PWM	Pulse Width Modulation
RLS	Recursive Least Square
RPM	Revolutions Per Minute
SMC	Sliding Mode Controller
VSS	Variable Structure Systems

2.2 Mechanics

Notations regarding mechanical part of the loader:

θ_1	lift/boom angular position
θ_2	tilt/bucket angular position
l_1	lift cylinder extension
l_2	tilt cylinder extension
c_1	cos (θ_1)
s_1	sin (θ_1)
c_{12}	cos ($\theta_1 + \theta_2$)
s_{12}	sin ($\theta_1 + \theta_2$)
τ_1	torque at joint 1
τ_2	torque at joint 2
$h_1(\theta_1)$	geometric transformation from boom angular position to lift cylinder extension [1]
$h_2(\theta_2)$	geometric transformation from bucket angular position to tilt cylinder extension [1]

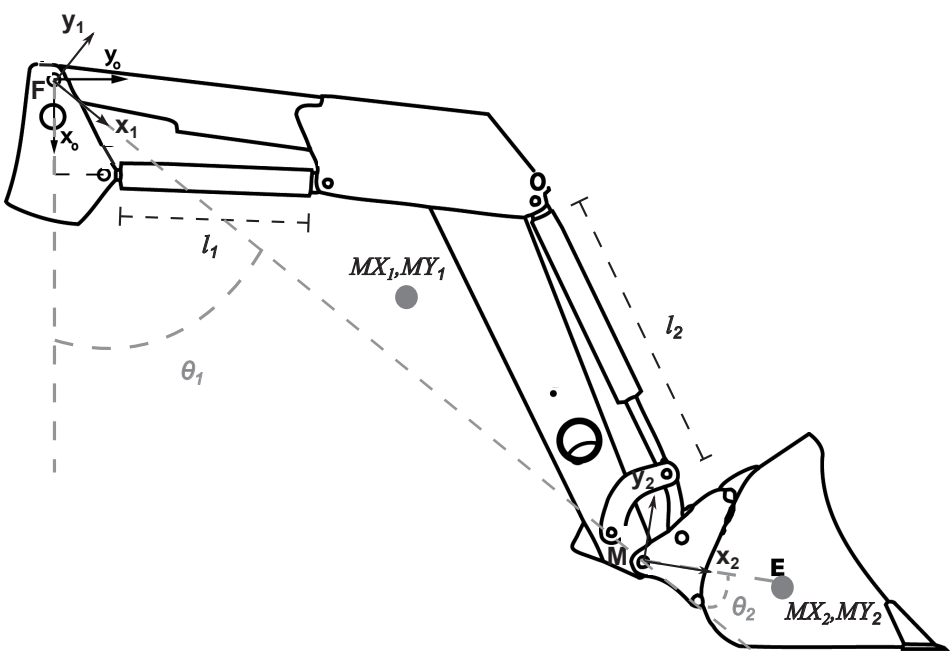

Fig. 2.1: The mechanical subsystem of the front-end loader under consideration with the assigned frames (x_1, y_1 and x_2, y_2)

$\overline{MX}_1$	center of gravity of boom structure[2] projected on x_1-coordinate
$\overline{MY}_1$	center of gravity of boom structure projected on y_1-coordinate
$\overline{MX}_2$	center of gravity of bucket structure[3] projected on x_2 - coordinate
$\overline{MY}_2$	center of gravity of bucket structure projected on y_2 - coordinate
$\overline{ZZ}_1$	moment of inertia of the boom around its center of mass
$\overline{ZZ}_2$	moment of inertia of the bucket around its center of mass

2.3 Hydraulics

Notations regarding hydraulic part of the loader are categorized into notations that are related to hydraulic cylinders and ones related to hydraulic valves.

2.3.1 Cylinders

Cylinders in Front-End Loaders get their flow supply from the tractor through hydraulic valves. Thus, a brief description of a simplified hydraulic valve used in this thesis is presented here. The valve is an open-center valve with parallel configuration (Fig. 2.2). An open center valve bypasses that at neutral position, i.e. $x_{s1} = 0$, $x_{s2} = 0$, the flow from the supply is returned to the tank (or power beyond). Other than neutral position, e.g. when one of the spool is not fully shifted ($0 < x_{s1} < \bar{x}_{s1}$), part of the total flow supply (q_{in}) goes to one cylinder chamber (q_{1b}) and the rest of the flow goes to the tank (q_{pb}) while the flow from the other cylinder chamber (q_{1a}) goes to the tank. Besides, a valve with parallel configuration has the supply connected to all 4-way upstream (inlet) sections and the tank connected to all the 4-way downstream (outlet) sections. The notations related to hydraulic cylinders are:

[1]The geometric transformations are derived in [34]

[2]The boom structure in this thesis is the structure that connects point F to point M in Fig. 2.1

[3]The bucket structure in this thesis is constituted of tool carrier and bucket, which will be simplified to bucket for the rest of the thesis

l_1	lift cylinder extension
p_{1a}	pressure at the piston side of lift cylinder
A_{1a}	area of the piston side of lift cylinder
V_{1a}	volume of the piston side of lift cylinder
p_{1b}	pressure at the rod side of lift cylinder
A_{1b}	area of the rod side of lift cylinder
V_{1b}	volume of the rod side of lift cylinder
l_2	tilt cylinder extension
$\overline{l_2}$	maximum tilt cylinder extension
$\overline{\dot{l}_2}$	maximum tilt cylinder velocity
$\underline{l_2}$	minimum tilt cylinder extension
p_{2a}	pressure at the rod side of tilt cylinder
A_{2a}	area of the rod side of tilt cylinder
V_{2a}	volume of the rod side of tilt cylinder
p_{2b}	pressure at the piston side of tilt cylinder
A_{2b}	area of the piston side of tilt cylinder
V_{2b}	volume of the piston side of tilt cylinder

f_h	hydraulic force
F_R	friction force
p_s	supply pressure
p_{pb}	pressure at power beyond
p_t	tank pressure
q_{1a}	flow to the piston side of lift cylinder
q_{1b}	flow to the rod side of lift cylinder
q_{2a}	flow to the rod side of tilt cylinder
q_{2b}	flow to the piston side of tilt cylinder
q_{pb}	flow to the rest of the hydraulic circuit, e.g. power beyond/tank
q_{in}	total flow from the pump
x_{s1}	lift spool displacement
x_{s2}	tilt spool displacement
$\overline{x_{s1}}$	maximum positive displacement of lift spool
$\overline{x_{s2}}$	maximum positive displacement of tilt spool

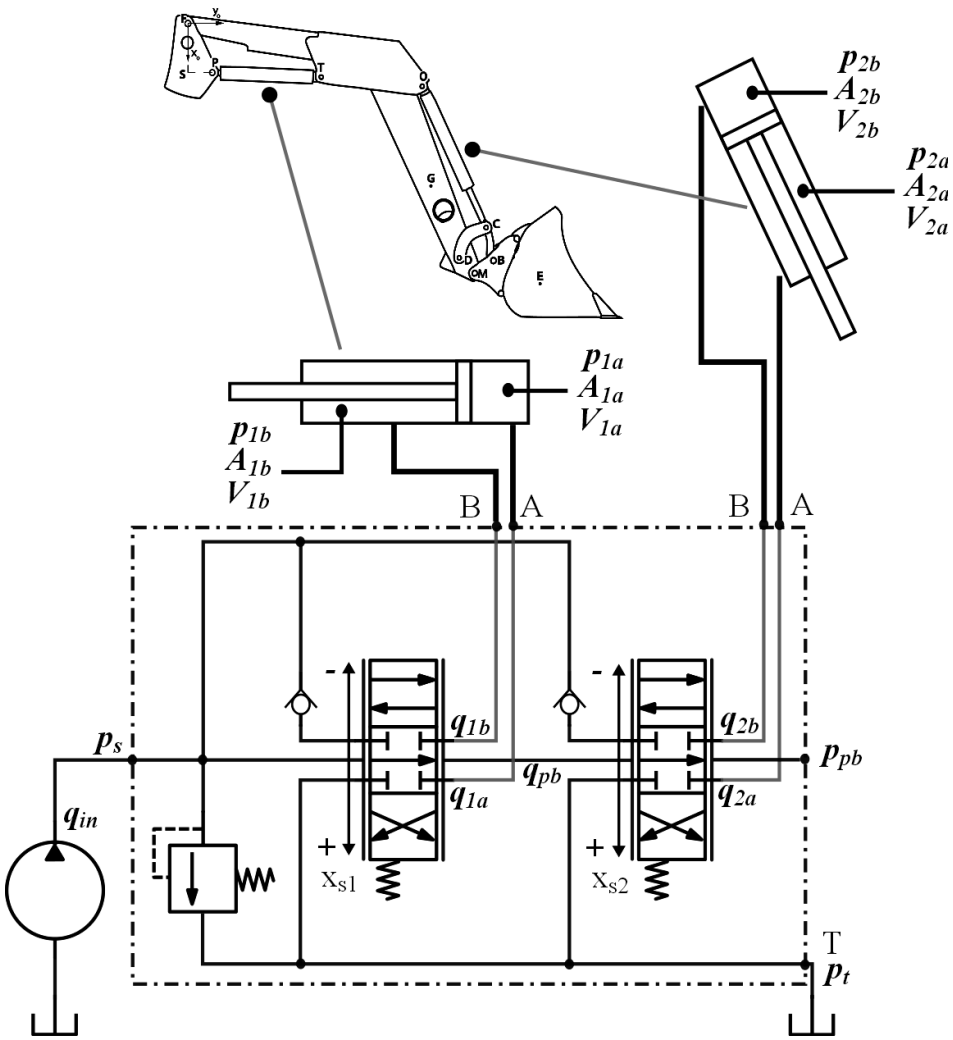

Fig. 2.2: A schematic diagram of a simplified hydraulic valve with parallel open-center configuration that is connecting the flow supply in a tractor to the cylinders of the mounted front-end loader.

2.3.2 Hydraulic Valve

A possible simplified physical construction of a parallel valve is shown in Fig. 2.3. It is a pilot operated solenoid valve, i.e. a small solenoid valve (called pilot) is actuating a larger main valve. The solenoid valve is omitted in Fig. 2.3 to be focus on the valve

coefficients of the main valve that will be used in this thesis. The notations related to the main hydraulic valve are:

C_d	discharge coefficient
c_{pb}	valve coefficient of the way to the power beyond
c_{2at}	valve coefficient of the way that connects rod side of tilt cylinder and tank
c_{2sa}	valve coefficient of the way that connects rod side of tilt cylinder and supply
c_{2sb}	valve coefficient of the way that connects piston side of tilt cylinder and supply
c_{2bt}	valve coefficient of the way that connects piston side of tilt cylinder and tank

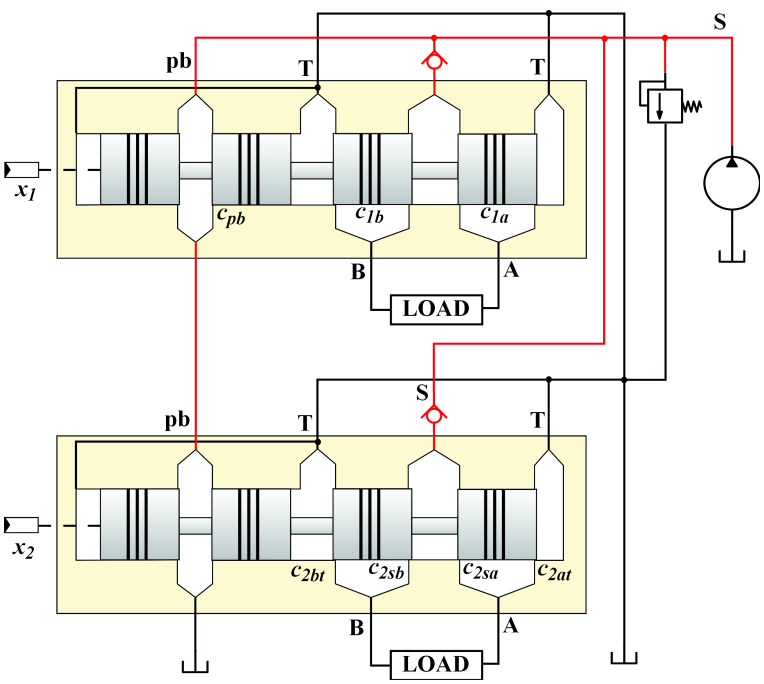

Fig. 2.3: One possible cutaway of a physical open center valve stack with parallel configuration adapted from [18].

c_{1a}	valve coefficient to the piston side of lift cylinder[5]
c_{1b}	valve coefficient to the rod side of lift cylinder[6]
u_1	current to the solenoid that shifts spool 1
u_2	current to the solenoid that shifts spool 2
$S_{2a}(x_{s2})$	tilt spool opening area to the rod side of tilt cylinder
$S_{2b}(x_{s2})$	tilt spool opening area to the piston side of tilt cylinder
$S_{1a}(x_{s1})$	tilt spool opening area to the piston side of lift cylinder
$S_{1b}(x_{s1})$	tilt spool opening area to the rod side of lift cylinder

[5]The coefficient c_{1a} is used when one assumes $c_{1at} = c_{1sa}$
[6]The coefficient c_{1b} is used when one assumes $c_{1bt} = c_{1sb}$

3 Modeling

Whenever control or simulation is of interest, modeling a system is necessary and it depends on the questions to be answered [33]. Two models are used for two tasks in this work. In the case of ESL, a model of a hydraulic cylinder is used to design a controller and to analyze the controller's performance. In the case of payload estimation, a mechanical model of this loader is mainly used.

For more general tasks, e.g. a realistic numerical simulation or simultaneous control of both cylinders, a model of hydraulics valve is required as both cylinders have a limited shared flow supply and varying pressure supply that depends on both spool displacements and the connected loads, which is not the case for some other similar systems such as forestry cranes [16, 17].

3.1 Hydraulics Cylinder

As the tilt motion, during manual control of the lift motion, is the control object in ESL task, a simplified model of the tilt hydraulic cylinder is used to design and to tune a controller for lowering motions (paper B). Assuming a known constant supply pressure and no pressure drop along the hoses, the flow through the spool orifice is [28, page 41], [45]:

$$q_{2a} = \begin{cases} c_{2a} S_{2a}(x_{s2}) \sqrt{p_s - p_{2a}}, & \text{for } x_{s2} \geq 0 \\ -c_{2a} S_{2a}(x_{s2}) \sqrt{p_{2a} - p_t}, & \text{for } x_{s2} < 0 \end{cases} \tag{3.1}$$

and

$$q_{2b} = \begin{cases} c_{2b} S_{2b}(x_{s2}) \sqrt{p_{2b} - p_t}, & \text{for } x_{s2} \geq 0 \\ -c_{2b} S_{2b}(x_{s2}) \sqrt{p_s - p_{2b}}, & \text{for } x_{s2} < 0 \end{cases} \tag{3.2}$$

with the assumption $S_{2a}(x_{s2}) = S_{2b}(x_{s2}) = S(x_{s2})$, the flow through orifice can be

rewritten as [45]

$$q_{2a} = c_{2a}\phi_{2a}S(x_{s2}) \tag{3.3}$$

$$q_{2b} = c_{2b}\phi_{2b}S(x_{s2}) \tag{3.4}$$

where $\phi_{2a} = \sqrt{p_s - p_{2a}}\frac{(\text{sign}(S(x_{s2})+1))}{2} - \sqrt{p_{2a} - p_t}\frac{(\text{sign}(S(x_{s2})-1))}{2}$ and $\phi_{2b} = \sqrt{p_{2b} - p_t}$ $\frac{(\text{sign}(S(x_{s2})+1))}{2} - \sqrt{p_s - p_{2b}}\frac{(\text{sign}(S(x_{s2})-1))}{2}$.

The flow entering the cylinder causes pressure dynamics that is governed by [28, page 53]:

$$\dot{p}_{2a} = \frac{\beta}{V_{2a}}\left(-\dot{V}_{2a} + q_{2a}\right) \tag{3.5}$$

$$\dot{p}_{2b} = \frac{\beta}{V_{2b}}\left(-\dot{V}_{2b} + q_{2b}\right) \tag{3.6}$$

Then, the generated hydraulic force is computed as follows

$$f_{h2} = p_{2a}A_{2a} - p_{2b}A_{2b} \tag{3.7}$$

in the domain

$$D = \{\underline{l_2} \le l_2 \le \overline{l_2}, \quad |\dot{l}_2| < \overline{\dot{l}_2}, \quad p_{2a}, p_{2b} \in (p_t, p_s), \quad |x_{s2}| < \overline{x_{s2}}, \quad q_{2a} < \overline{q_2}\} \tag{3.8}$$

which is ensured by the mechanical structure, safety valves in the system and limited available flow supply. Outside of this domain, the hydraulic force is uncertain.

Differentiating this force with respect to time, substituting expressions (3.3)-(3.6) and collecting similar terms results in a first order model [45] that is used for analysis in papers A and B:

$$\dot{f}_{h2} = -\eta\dot{l}_2 + \phi\Psi(u_2) \tag{3.9}$$

where Ψ denotes input nonlinearity of the hydraulic valve (Fig. 3.1), and η and ϕ are defined as follows

$$\eta = \beta\left(\frac{A_{2a}^2}{V_{2a}(l_2)} + \frac{A_{2b}^2}{V_{2b}(l_2)}\right) \tag{3.10}$$

$$\phi = \beta\left(\frac{c_{2a}A_{2a}\phi_{2a}}{V_{2a}(l_2)} + \frac{c_{2b}A_{2b}\phi_{2b}}{V_{2b}(l_2)}\right) \tag{3.11}$$

The values of η and ϕ are bounded in D so that $0 < \underline{\phi} < \phi < \overline{\phi}$ and $0 < \underline{\eta} < \eta < \overline{\eta}$ with some constant bounds. For this reason, a first order nonlinear differential equation can

represent the tilt cylinder dynamics with the derivative of hydraulic force representing a bounded perturbation:

$$\dot{l}_2 = \frac{\phi}{\eta}\Psi(u_2) - \frac{1}{\eta}\dot{f}_{h2}. \tag{3.12}$$

Moreover, this quotient is always positive in D.

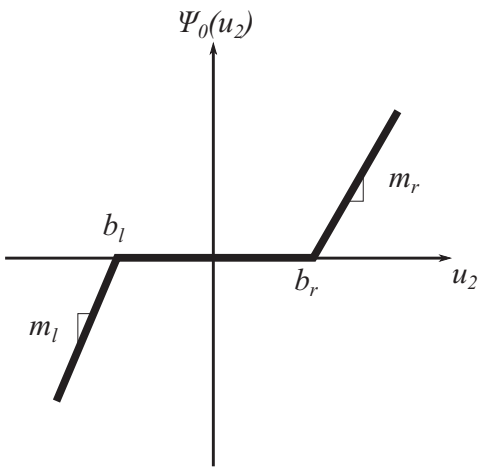

Fig. 3.1: An example of dead zone input nonlinearity [43]. Outside of the dead zone region (b_l to b_r), it is assumed that increment of the opening area is proportional to the input current with gradient m_l and m_r

Different models, both linear and non-linear, have been presented and used for control design and analysis of a hydraulic cylinder. Several works utilizing a linearized model are done to analyze the robustness of PI controller for a hydraulic actuator [37] and to design a robust controller [35] or an adaptive controller [7]. Several works based on nonlinear model are done with design of non-linear controller [21, 41]. Here a non-linear model is employed because we are interested in the whole working region, e.g. the whole range of cylinder extension, different loads and different velocities within D due to different lifting/lowering velocities.

3.2 Mechanics

The mechanical part of this loader can be modeled as a planar 2-DOF manipulator assuming negligible pressure difference in the left and right arms. For this manipulator, the

Table 3.1: Modified DH parameters

joint	α_j	d_j	θ_j	r_j
1	0	0	θ_1	0
2	0	$\overline{FM}$	θ_2	0
ee	0	$\overline{ME}$	0	0

generalized coordinates are chosen as height, h, and bucket orientation angle, γ, since this choice is the most convenient for ESL task description: we would like to keep γ constant when the driver changes h manually by controlling the lift cylinder.

With the frame assignment as in fig. 3.2, the modified DH-convention parameters [20] are given in table 3.1 and the loader forward kinematics are given in (3.13) - (3.14).

$$h = h_0 - (\overline{FM}c_1 + \overline{ME}c_{12}) \tag{3.13}$$

$$\gamma = \theta_1 + \theta_2 - 90 \tag{3.14}$$

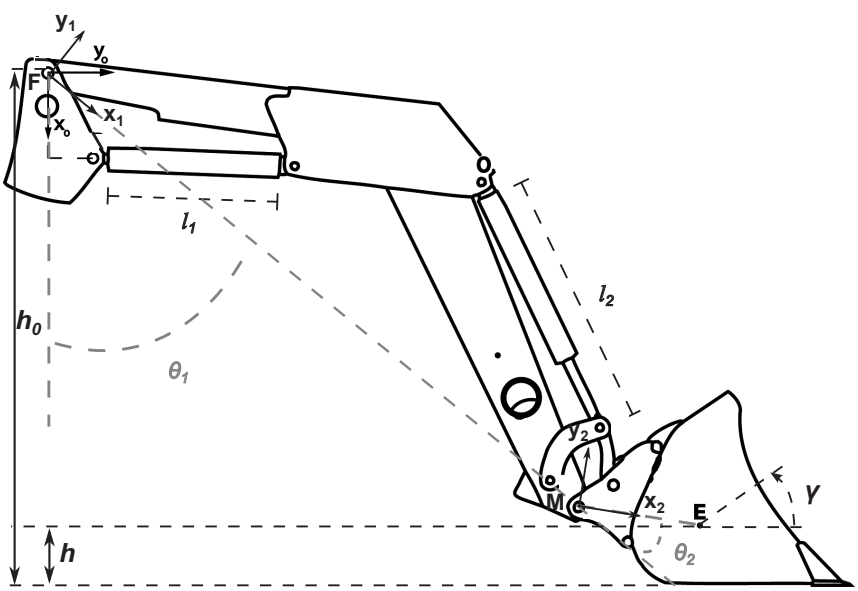

Fig. 3.2: A front-end loader under consideration with assigned frames.

Based on Table 3.1, the system dynamics, written with respect to the joint variables, is:

$$A(\boldsymbol{\theta})\ddot{\boldsymbol{\theta}} + C(\boldsymbol{\theta}, \dot{\boldsymbol{\theta}})\dot{\boldsymbol{\theta}} + \boldsymbol{G}(\boldsymbol{\theta}) + \boldsymbol{Fr}(\dot{\boldsymbol{\theta}}) = \boldsymbol{\tau}, \tag{3.15}$$

where the inertia $A(\boldsymbol{\theta})$, Coriolis $C(\boldsymbol{\theta}, \dot{\boldsymbol{\theta}})$, gravity $\boldsymbol{G}(\boldsymbol{\theta})$ and friction terms $\boldsymbol{Fr}(\dot{\boldsymbol{\theta}})$ of the loader are presented as follows:

- Components of inertia matrix $A(\boldsymbol{\theta}) = \begin{bmatrix} A_{11} & A_{12} \\ A_{21} & A_{22} \end{bmatrix}$:

$$\begin{aligned} A_{11} &= M_2\overline{FM}^2 + 2M_2\overline{FM}\left(c_2\overline{MX}_2 - s_2\overline{MY}_2\right) + M_1\overline{MX}_1^2 \\ &\quad + M_2\overline{MX}_2^2 + M_1\overline{MY}_1^2 + M_2\overline{MY}_2^2 + \overline{ZZ}_1 + \overline{ZZ}_2 \\ A_{12} &= M_2\overline{MX}_2^2 + M_2\overline{MY}_2^2 + M_2\overline{FM}\left(\overline{MX}_2 c_2 - \overline{MY}_2 s_2\right) + \overline{ZZ}_2 \\ A_{21} &= A_{12} \\ A_{22} &= M_2\left(\overline{MX}_2^2 + \overline{MY}_2^2\right) + \overline{ZZ}_2 \end{aligned}$$

- Components of Coriolis matrix $C(\boldsymbol{\theta}, \dot{\boldsymbol{\theta}}) = \begin{bmatrix} C_{11} & C_{12} \\ C_{21} & C_{22} \end{bmatrix}$:

$$\begin{aligned} C_{11} &= -M_2\dot{q}_2\overline{FM}\left(\overline{MY}_2 c_2 + \overline{MX}_2 s_2\right) \\ C_{12} &= -M_2\,\overline{FM}\,\left(\dot{\theta}_1 + \dot{\theta}_2\right)\left(\overline{MY}_2 c_2 + \overline{MX}_2 s_2\right) \\ C_{21} &= M_2\,\overline{FM}\,\dot{\theta}_1\left(\overline{MY}_2 c_2 + \overline{MX}_2 s_2\right) \\ C_{22} &= 0 \end{aligned}$$

- Components of gravity vector $\boldsymbol{G}(\boldsymbol{\theta}) = \begin{bmatrix} G_1 \\ G_2 \end{bmatrix}$:

$$\begin{aligned} G_1 &= g\left(M_2\overline{MY}_2 c_{12} + M_2\overline{MX}_2\, s_{12} + M_1\overline{MY}_1\, c_1 + M_2\overline{FM} s_1 + M_1\overline{MX}_1 s_1\right) \\ G_2 &= M_2 g\left(\overline{MY}_2 c_{12} + \overline{MX}_2 s_{12}\right) \end{aligned}$$

- Friction $Fr(\dot{\boldsymbol{\theta}}) = \begin{bmatrix} F_{cl1} + F_{v1}\dot{\theta}_1 \\ F_{cl2} + F_{v2}\dot{\theta}_2 \end{bmatrix}$

where $\theta_{1,2}$ are the angular positions of the joints, $\dot{\theta}_{1,2}$ are the angular velocities of the joints, F_{cli} and F_{vi} are Coulomb friction and viscous friction coefficients respectively, $s_i = \sin(\theta_i)$, $c_i = \cos(\theta_i)$, i = 1,2, $s_{12} = \sin(\theta_1 + \theta_2)$, $c_{12} = \cos(\theta_1 + \theta_2)$, and $\overline{FM}$ is one of geometric parameters of a loader (see Fig. 3.2).

A simplified mechanical model, with only gravitational torque, is used in the payload estimation task [Paper C & D].

3.3 Hydraulic Valve

For more general tasks, such as simulation or executing synchronized motion of both cylinders, the interaction in the hydraulic valve stack should be taken into account. A valve-controlled system with constant flow is dealt with here, specifically a 6-way open center valve, where the flow is continuously directed to the tank when all the spools are in neutral [14], with overlap land (closed center valve in [28, page 78]). The valve stack, constituted by two spools that control boom and bucket motions, is connected in parallel. Fig. 3.3 shows an example of a basic valve with parallel OC circuit, where the supply is connected to all the functions [18]. In this system, the supply pressure is not constant. The supply pressure is built to overcome the load pressure to initiate the flow. Thus, a model of supply pressure is investigated below. Note that a different valve is used here in modeling the supply pressure[1]. The valve that is used in this experiment is a basic valve with known opening areas for the corresponding spool displacements without additional pressure compensator feature.

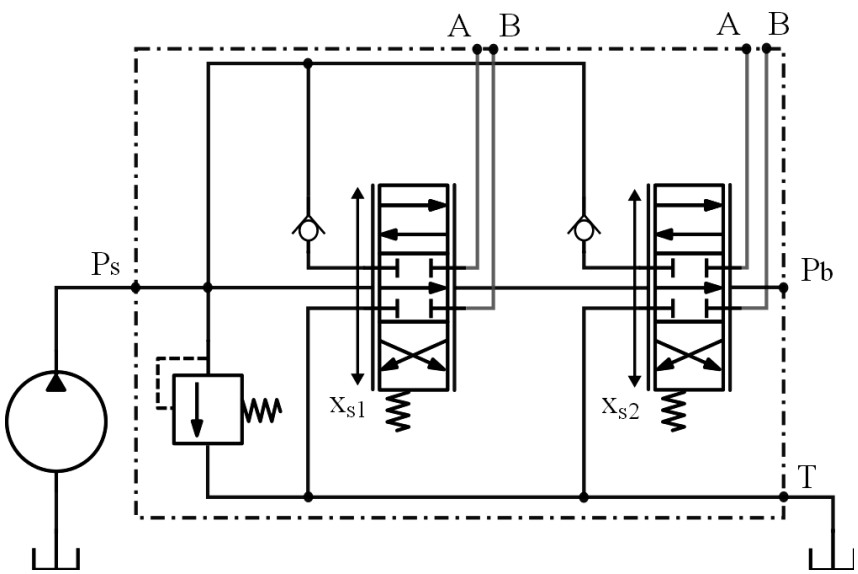

Fig. 3.3: An example of a parallel open-center valve (adapted from [18])

[1]There are two different valves that have been investigated in this thesis: the solenoid pilot-operated valve and the stepper motor valve. The first valve is used as the base for the ESL and payload estimation tasks. However, the mapping from spool extension to the opening areas is not available with this valve. The latter valve has this mapping such that the investigation of supply pressure built-up is possible

In the case when one function is activated, i.e. one spool is shifted, the spool displacement will increase the opening area of the orifice that is connected to a cylinder chamber and reduce the opening area that is connected to the power beyond at the same time [38, page 14]. In this case, the flow supply is connected to both the cylinder chamber and power beyond, and the pressure supply can be analytically computed by solving the flow conservation expression (Eq. 3.16) for lowering motion, provided we know the opening areas, discharge coefficient and fluid density. The discharge coefficient and fluid density used in this analysis are 0.6 and 870 kg/m^3.

$$\begin{aligned} q_{in} &= q_{1b} + q_{pb} \\ &= c_{1b} S_{1b}(x_{s1}) \sqrt{p_s - p_{1b}} + c_{pb} S_{pb}(x_{s1}) \sqrt{(p_s - p_{pb})} \end{aligned} \tag{3.16}$$

A set of lowering motions has been executed to verify this relation. The cylinder extensions and pressure measurements have been recorded. Two different pressure sensors are installed. The sensors at the supply and power beyond, p_s and p_{pb} have an accuracy of 1.5 bars. The one at the cylinder chamber, p_{1b}, has an accuracy of 4 bars.

Figure 3.4a shows the comparison between the supply pressure measurement and the one computed based on the flow conservation expression (Eq. 3.16). Most of the computed supply pressures, taking into account the sensors accuracy, lie within the measured supply pressures except for several maximum displacements. With bigger spool displacement, the neglected pressure drop along the passage is higher as the fluid velocity is higher. In addition to similar supply pressure profile, the flow profile with respect to spool displacements that is computed based on analytical supply pressure also corresponds to the flow profile that is based on the velocity estimation of cylinder motion (Fig. 3.4b). This indicates that the flow conservation explains the supply pressure build-up in the hydraulic valve.

However, this analytical solution becomes more involved when both functions are activated, that is when both spools are not in positions to completely block the flow. A numerical solution is required to compute the supply pressure, which might be required for simulation and optimizing a synchronized motion of both cylinders. No further work towards this direction has been performed since this has not been found useful for improving performance of ESL and load estimation algorithms proposed in this thesis.

While the supply pressure has not been built enough to overcome the load pressure, the check valve prevents the flow back from the load to the pump. This causes a considerable delay from the time a command is applied to the time the expected motion is observed. In the system we have been working for ESL and payload estimation tasks, the valve has an

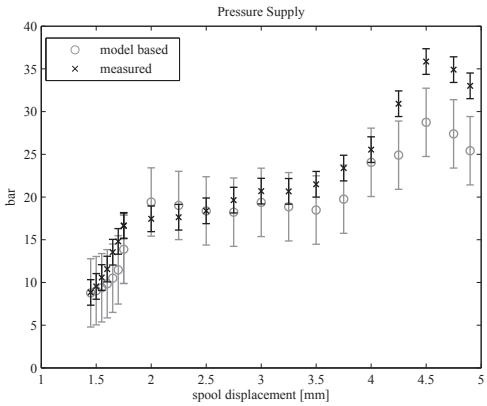

(a) Comparison between the model based supply pressure p_s and its measurement

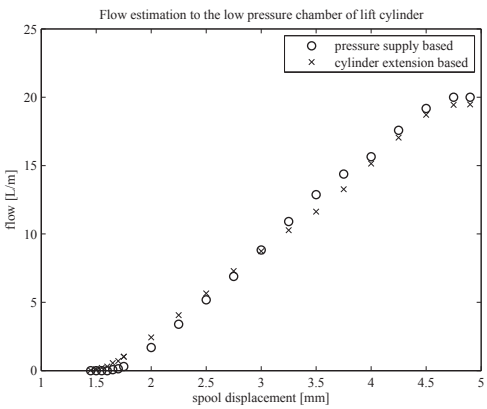

(b) Comparison of the flow estimation based on pressure supply model and the one based on estimated cylinder velocity

Fig. 3.4: Verification of flow conservation in a parallel open-center valve to compute the supply pressure

inlet pressure compensator. This reduces the delay and prepare the system with a constant pressure difference.

With a constant pressure difference, the steady-state flow only depends on the spool opening according to Eqn. (3.1, 3.2). The steady state flow profile of this valve with

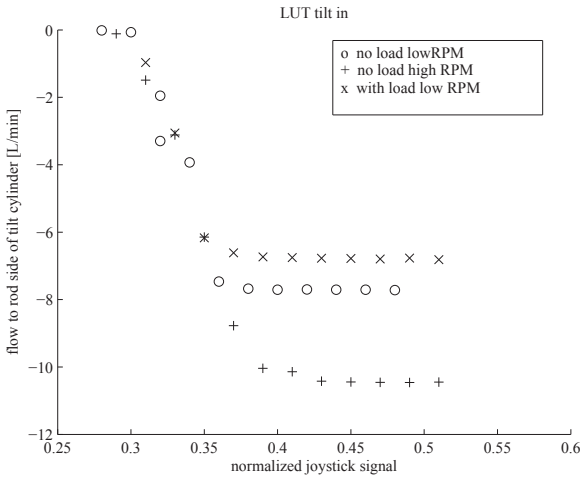

Fig. 3.5: Steady state flows with respect to current commands of tilt-in motion from the valve with inlet pressure compensation

respect to the normalized current command for tilt-in motion is shown in Fig. 3.5. A linear relation between increments is observed between the dead-zone and saturation. Moreover, the saturation is observed at different levels of current commands for different RPM settings.

The driver controls the flow supplies by changing the RPM settings. The saturation profile in Fig. 3.5 will change when both spools are activated as well as when other functions in the tractor are activated. This is because the flow supply is shared to all the functionalities of the tractor, e.g. traction and the attached FEL.

4 Electronic Self Leveling (ESL)

For many common agricultural operations, a two-degree-of-freedom (2-DOF) Front-End Loader (FEL), attached to a tractor, must preserve the initial orientation of the attached implement during lifting and lowering motions as one of the desired features [32]. The self-leveling task can be realized mechanically or hydraulically with several limitations [23]. In the same work, an electronic solution based on feed forward is proposed for a particular linear valve with a known tractor supply. A recently released product is available for a proprietary tractor [12], where tractor condition is possibly available. Here, an electrical solution to realize this task, based on closed-loop control for a particular valve, is investigated where no information is available about different possible tractors to be mounted on.

As a highly nonlinear system, nonlinear model-based controllers have been reported to perform better than linear controllers for hydraulic systems [27]. Besides, as other mobile hydraulic systems, FELs are expected to work in a highly uncertain environment. Thus, robustness is important such that controllers that can deal with uncertainties and perturbations are considered.

In this work, the disturbance is mainly introduced by the driver who manually controls the boom motion. Hence, the ESL task becomes a problem of the automatic tilt cylinder control under an arbitrary motion of the lift cylinder. Our goal is to automatically maintain the implement angular position with respect to a world frame or a frame fixed on an attached tractor under the influence of the main disturbance. This task is considered in Paper A and Paper B, while here we provide some additional details and related discussions. Moreover, investigation on one possible fault and the mitigation proposal are presented in section 4.2. Lastly, the background theories related to control design are presented in

section 4.3.

4.1 Controllers

To compare different controllers, we have built a simulation model that is constituted by hydraulics dynamics and the equations of motion presented in Chapter 3. Due to the high complexity of the unmodeled augmented variety of the stack valve, e.g. inlet pressure compensator and flow regeneration modules, a simplified hydraulic circuit containing two identical hydraulic cylinders with two constant pressure supplies is used in simulation. Hydraulics parameters from the CAD model are utilized together with the valve coefficients and bulk modulus presented in Table 4.1:

Table 4.1: Valve coefficients and bulk modulus parameters for simulation

symbol	description	value
c_{sa}	supply to chamber-a coefficient	3.9×10^{-7} $\mathrm{m}^{3.5}\mathrm{kg}^{-1}$
c_{bt}	chamber-b to tank coefficient	2.9×10^{-7} $\mathrm{m}^{3.5}\mathrm{kg}^{-1}$
c_{sb}	supply to chamber-b coefficient	5.6×10^{-7} $\mathrm{m}^{3.5}\mathrm{kg}^{-1}$
c_{at}	chamber-a to tank coefficient	4.8×10^{-7} $\mathrm{m}^{3.5}\mathrm{kg}^{-1}$
β	bulk modulus	1.7×10^{9} MPa

Note that the valve coefficients in (3.1) and (3.2) now have different values depending on which chamber the supply or the tank is connected to [2]. Similar procedure to obtain the valve coefficients can be followed when the supply pressure measurement is available. In the simulation, these valve coefficients are set the same for lift and tilt cylinders.

With this simplified system, a standard linear controller (PI) and a perturbation compensation method, Sliding Mode Control, have been compared to realize ESL. A PI controller is chosen since it might give a zero steady state error for a type I system under a constant velocity disturbance [37]. The Sliding Mode Control was found to be one of the best controllers for a similar heavy-duty manipulator in mining industry [8]. Other leading controllers are Acceleration Feedback using an experimentally Identified Friction Model (FRID) and Model Reference Adaptive Controller (MRAC). However, it is expected that friction varies considerably in a wide range of temperatures where the loaders are typically operated such that identifying a thorough friction model might be a time-consuming procedure. On the other hand, the expected real-time implementation with ECU might require unavailable memory and computational resources to implement MRAC.

In simulation, the deadzone compensation is perfectly set such that the comparison of controllers is focused on compensating the disturbance from the driver, which is the lowering or lifting velocity. A pulse signal is applied to the first cylinder in open loop to simulate a driver's aggressive motion control and hence introducing the disturbance to the system. The linear controller is tuned by trial and error to achieve a certain performance, e.g. 0.5 degree tracking error for lifting and 1 degree tracking error for lowering. The classical first order Sliding Mode Controller is also tuned by trial and error.

It is observed that a high gain proportional term will reduce the tracking error to ensure the desired performance, but more oscillations are observed in lifting motion (Fig. 4.1 during the first 5 seconds). However, a better performance in lowering motion is observed without much oscillation as well as lower error during transient. Increasing the integral gain will reduce the error during the motion achieving a better steady-state error. However, a windup effect is observed at lift stationary condition which cannot be solved with anti windup module from MATLAB. As the constant velocity disturbance is not present at stationary condition, it is not clear what integral term is fighting for. On the other hand, with disturbance compensation, e.g. using sliding mode term, a certain performance can be achieved without exciting longer oscillation or windup effect (Fig. 4.2b).

From the simulation results, similar comparison has also been done in experiments that are reported in Paper A. The comparison has been done at a certain working condition: low RPM and an empty bucket as an implement. The controllers are tuned by trial and error: the gains are gradually increased within certain reasonable ranges, until no performance improvement and higher amplitude of oscillations are observed.

It is observed that different controllers are required for lifting and lowering motion. A linear controller is enough to maintain ESL in lifting motion. Whereas, a stronger controller, in the form of additional practical disturbance compensation in this work, is required to maintain sufficiently accurate ESL in lowering motion. In lowering, successful ESL requires tilting the bucket in the direction opposite to the influence of the gravity. Conversely, the gravity helps the tilt out motion to maintain ESL during lifting.

From the modeling viewpoint, the gravity influence can be analyzed from the simplified dynamic model (3.12) derived in Chapter 3 (see also Paper A):

$$\dot{l}_2 = \frac{\phi}{\eta}\Psi(u_2) - \frac{1}{\eta}\dot{f}_{h2}.$$

The function in the numerator ϕ, which amplifies the impact of control signal u_2 is larger in tilt out motion due to larger pressure difference, $p_{2a} - p_t$ and $p_s - p_{2b}$, than in tilt in

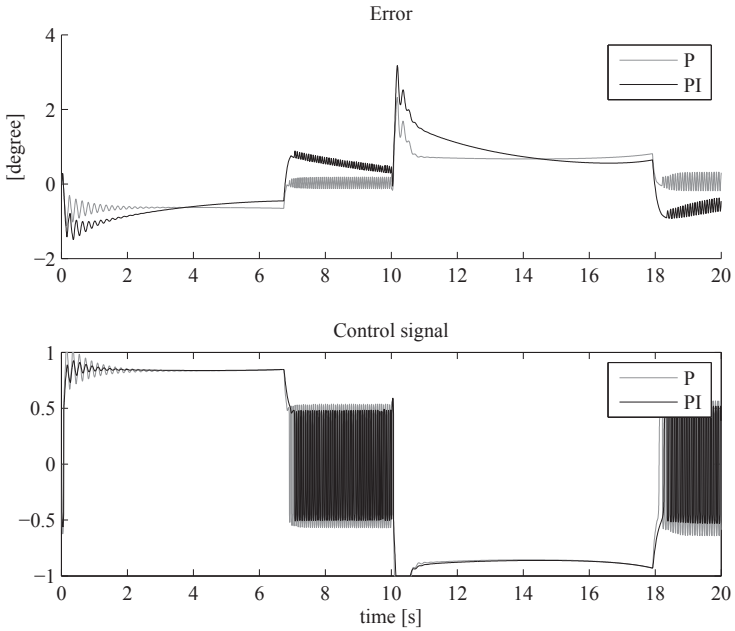

Fig. 4.1: Comparison of controllers performance between P and PI in simulation

motion, $p_{2b} - p_t$ and $p_s - p_{2a}$ in the presence of an inlet pressure compensator. Whereas, the denominator, η, is the same at the same cylinder extension regardless the lifting or lowering motion.

Moreover, while Sliding Mode Control gives a good control performance in simulation, chattering is visible in experiment[1]. This leads us to explore Active Disturbance Rejection Control (ADRC) that compensates the disturbance based on its estimation instead of worse-case-disturbance-based-scenario aggressive domination by SMC. Thus, we compare different controller schemes investigating the importance of dead zone compensation, linear controller, SMC and ADRC. It turns out that the scheme that combines SMC and ADRC is able to reach the desired error with less oscillation that is observed in lowering motions which is reported in Paper A. This result has motivated us to propose a tuning procedure of a controller with this scheme for lowering motions.

This tuning procedure has been reported in Paper B. We base our analysis on a nonlinear model of a hydraulic cylinder as the cylinder is expected to work in the whole

[1]Different SMC variants have been investigated as well, namely Super Twisting, [25], Exponential SMC and SMC with varying gain, [44]. However, similar oscillation behavior has been observed.

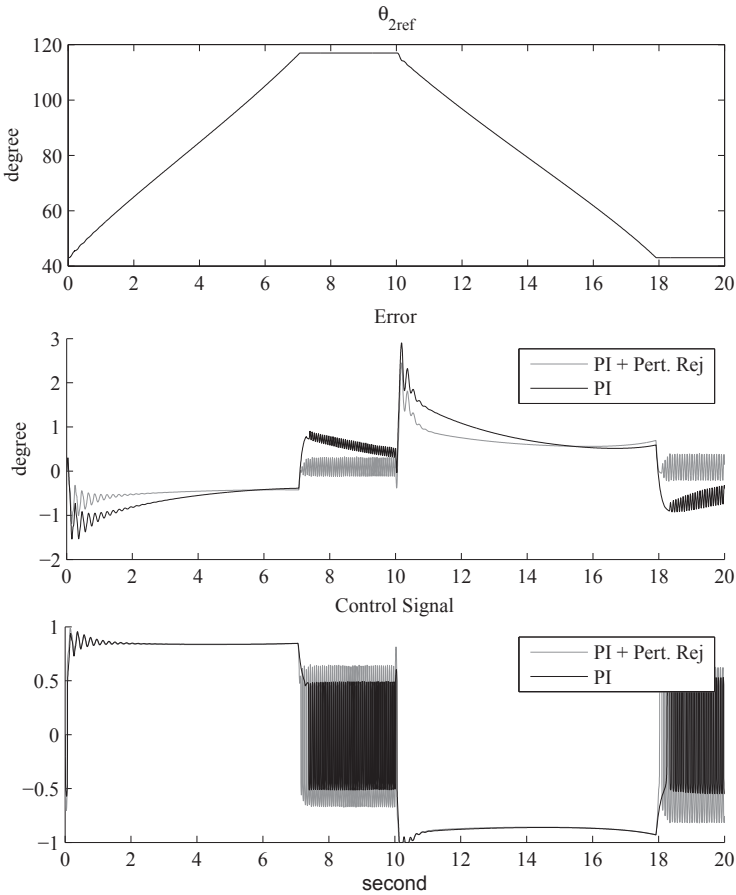

Fig. 4.2: Comparison of controllers performance between PI and PI with Pert. Rej. in simulation

range of extensions, various loads and different velocities. Due to a limited commutation frequency of the hydraulic actuator, an ideal sliding mode can not be induced. Thus, the discontinuous SMC term is now considered as a relay controller whose action does not need to overcome the disturbances. The tuning procedure is now proposed for a controller combining proportional, disturbance observer and a relay controller. Based on a Vector Lyapunov function (see Section 4.3.2), a set of parameters has been obtained to achieve a steady-state error less than the requested two degrees. It has been implemented in a

prototype setup at the company and compared to a PI controller.

In addition, a procedure to tune the controller parameters, a safeguard function is developed to deal with a possible flow limitation (see Section 4.2). From the control design perspective, this is a saturation problem. The saturation level varies depending on the level of RPM. The problem is more critical in lowering motion than in lifting because, roughly speaking, the fluid prefers to go to the low pressure chamber, which assists the lowering motion but hesitates to fill the high pressure chamber to perform the tilt-in motion. Intuitively, reducing the boom command, which will reduce the flow consumption by the prioritized lifting cylinder, should be done. Here, an idea to reduce the commanded boom velocity from the tilt information on maintaining ESL is proposed based on properties of the mechanical model. By relying the analysis on the mechanical part, the detailed description of a complex hydraulic model is not required and the focus is on the task.

4.2 Dealing with insufficient flow

Maintaining ESL during the lowering motion can be translated into filling the low pressure chamber of the lift cylinder and the high pressure chamber of the tilt cylinder. The boom command sent by a driver will determine the boom cylinder velocity and subsequently the required tilt cylinder velocity for compensation. With the information of the cylinders' chamber areas, the total required flow can be computed.

As the total flow is computed in cylinder domain, the idea is to convert the ESL condition expressed in the angular domain, $\theta_2 = c - \theta_1$, to a necessary condition in the cylinder domain as follows:

$$\dot{\theta}_2 = -\dot{\theta}_1 \tag{4.1}$$

$$\frac{\partial h_2(x_2)}{\partial x_2}\dot{x}_2 = -\frac{\partial h_1(x_1)}{\partial x_1}\dot{x}_1 \tag{4.2}$$

$$\frac{\partial h_2(x_2)}{\partial x_2}\dot{x}_2\frac{A_{a2}}{A_{a2}} = -\frac{\partial h_1(x_1)}{\partial x_1}\dot{x}_1\frac{A_{b1}}{A_{b1}} \tag{4.3}$$

$$r_{ref} = \frac{Q_{a2}}{Q_{b1}} = -\frac{A_{a2}}{A_{b1}}\frac{\partial h_1(x_1)}{\partial x_1}\left(\frac{\partial h_2(x_2)}{\partial x_2}\right)^{-1} \tag{4.4}$$

Differentiating ESL condition gives us a necessary condition on the angular velocity (4.1) and the cylinder velocity (4.2) by exploiting the geometric transformation. Multiplying by the corresponding cylinders' areas (4.3) and collecting terms together result in a derivation of the required flow ratio (4.4).

This ratio depends on the cylinders' areas, which are constant, and cylinders' extensions. Theoretically, every lift cylinder extension has one-to-one relation to the tilt cylinder extension in maintaining a certain bucket angle in the world frame. Thus, this ratio only depends on the lift cylinder extension (or lift angular position) to maintain a certain desired bucket angle.

When the total available flow is known, the time optimal trajectory of lift cylinder velocity is shown in Fig. 4.3 for a horizontal bucket angle ($c = \pm 88$ degree with respect to the assigned world frame). It shows that the time optimal trajectory is a non-constant lift cylinder velocity due to the effect of the non-linear geometric transformation. When the total available flow is unknown, this ratio can be used as a reference of succesful ESL in on-line application.

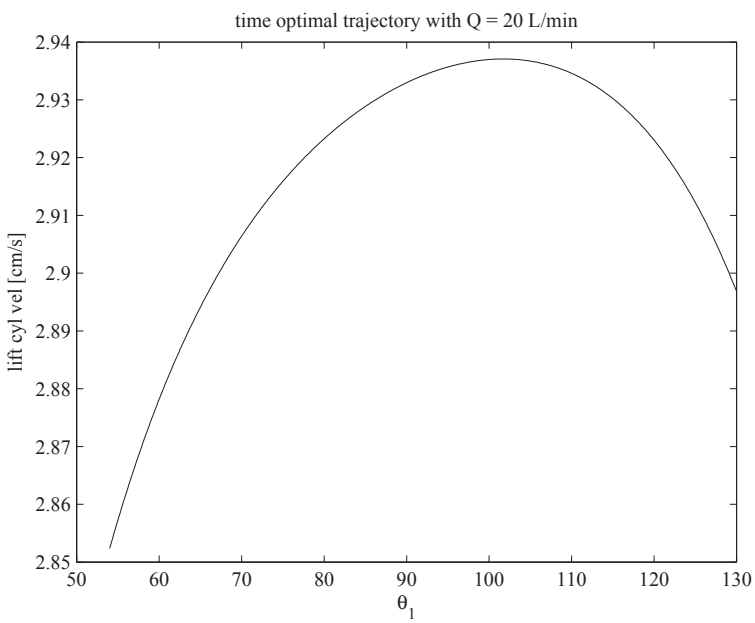

Fig. 4.3: The time optimal trajectory of lift cylinder velocity to maintain ESL at horizontal position (88 degrees) given the flow supply equals to 20 L/min

In online application, the actual flow ratio can be computed based on the estimated

cylinder velocities[2]:

$$r_{act} = \frac{Q_{a2}}{Q_{b1}} = -\frac{A_{a2}}{A_{b1}} \frac{\hat{\dot{x}}_2}{\hat{\dot{x}}_1}. \tag{4.5}$$

When there is enough flow supply, the quotient of the actual ratio and the reference ratio will be equal to 1. Whereas, when a flow supply shortage occurs, this quotient will be less than 1. The difference will be higher when further shortage occurs, which makes it a good feedback variable to reduce the boom command.

An implementation of using the quotient of flow ratio as a feedback variable to reduce boom commands has been carried out and tested on the experimental set-up without bucket. The difference of flow ratio from 1

$$r_{\text{difference}} = 1 - \frac{r_{act}}{r_{ref}}$$

is then multiplied by a constant before being used to smoothly reduce the lift command. Reducing lift command will automatically improve the ratio difference, and hence lower the reduction. The lift command that is detected at the maximum reduction is then set to be a new saturation level.

The proposed algorithm is able to detect different maximum boom lowering commands for different available flow supplies (Fig. 4.4). In the case of low RPM, the suggested saturation is -0.3122, which indicates a less lowering velocity than the suggested saturation in high RPM case, which is -0.3593. Moreover, the reduction is larger in the low RPM case due to a worse flow shortage than in the high RPM case, which can be indicated by a bigger maximum error in low RPM case.

Though the proposed method is working fine (with the current implementation) to find the saturation level, and hence the available flow, by reducing the boom command, the mechanism to detect excess flow followed by a mechanism to increase the actual level of saturation is not part of the proposal. Thus, increasing the cycle time when a driver increases the RPM setting in the middle of lowering motion is not possible with the proposed method.

4.3 Background Theory

4.3.1 Nonlinear Systems

As a nonlinear system of ordinary differential equations is decided to be the base of the work with Electronic Self Leveling, the stability analysis is done using a Lyapunov func-

[2] A differentiator is designed for this purpose, see section 6.2

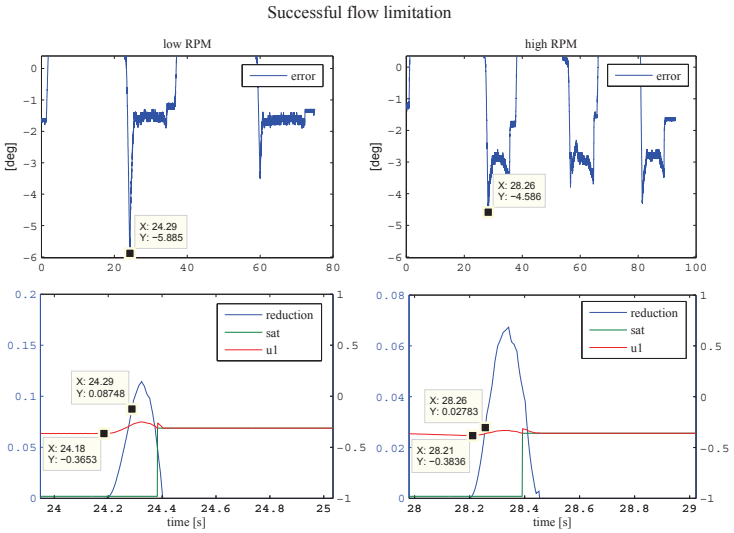

Fig. 4.4: Different detected saturation levels of boom lowering command for different RPM settings.

tion. With this tool, examining the derivative of certain functions along the trajectories of the system can determine the stability of the system through the stability of its equilibrium points, i.e. the property of the solutions initiated sufficiently close to the equilibrium to stay in its vicinity, instead of solving the equations. The decription below is based on [19, Chapter 4].

The equilibrium point $x = 0$ of a time varying system,

$$\dot{x} = f(t, x) \tag{4.6}$$

is **uniformly stable** if there exists a class κ function[3] α and a positive constant c, independent of t_0, such that

$$\|x(t)\| \leq \alpha(\|x(t_0)\|), \quad \forall t \geq t_0 \geq 0, \quad \forall \|x(t_0)\| < c.$$

The stability analysis using Lyapunov function is based on the following theorem:

Theorem 1 (Lyapunov)**.** *Let the origin $x = 0$ be an equilibrium point of $\dot{x} = f(t, x)$, i.e. $f(t, 0) = 0$, and $D \subset R^n$ be a domain containing $x = 0$. Suppose $f(t, x)$ is piecewise*

[3] A class κ function is a scalar continuous function $\alpha(r)$, that is strictly increasing and $\alpha(0) = 0$.

continuous in t and locally Lipschitz in x for all $t \geq 0$ and $x \in D$. Let $V(t,x)$ be a continuously differentiable function such that

$$W_1(x) \leq V(t,x) \leq W_2(x) \tag{4.7}$$

$$\frac{\partial V}{\partial t} + \frac{\partial V}{\partial x} f(t,x) \leq 0 \tag{4.8}$$

for all $t \geq 0$ and $x \in D$, where $W_1(x)$ and $W_2(x)$ are continuous positive definite[4] *functions on D. Then, the origin is uniformly stable.*

The solution of system (4.6) is **uniformly ultimately bounded with ultimate bound** d if there exists a positive constant c, independent of t_0, and for every $a \in (0,c)$, there is $T \geq 0$, dependent on a and d but independent of t_0, such that

$$\|x(t_0)\| \leq a \Rightarrow \|x(t)\| \leq d, \quad \forall t \geq t_0 + T. \tag{4.9}$$

In a particular case where the system is linear with a time and state dependent but bounded perturbation,

$$\dot{x} \quad = \quad Ax + g(t,x),$$

where A is Hurwitz and the perturbation is bounded $\|g(t,x)\| \leq \gamma$, a Lyapunov function can be chosen as

$$V(x) = \frac{1}{2} x^T P x$$

with $Q = Q^T > 0$ and P computed as the solution of the Lyapunov equation $PA + A^T P = -2Q$. This Lyapunov function satisfies

$$\frac{1}{2}\lambda_{\min}(P)\|x\|^2 \leq V(x) \leq \frac{1}{2}\lambda_{\max}(P)\|x\|^2$$

and its derivative along the system trajectories is constituted by:

$$\begin{aligned} \dot{V} &= \frac{1}{2}\left[x^T(PA + A^T P)x\right] + x^T P g \\ &= -x^T Q x + x^T P g \end{aligned}$$

such that

$$\begin{aligned} \dot{V}(t,x) &\leq -\lambda_{\min}[Q]\|x\|^2 + \|P\|\gamma\|x\| \\ &\leq -\frac{2\lambda_{\min}[Q]}{\lambda_{\max}[P]} V + \frac{2^{\frac{1}{2}}}{\lambda_{\min}^{\frac{1}{2}}[P]} V^{\frac{1}{2}} \|P\gamma\| \end{aligned}$$

[4] A positive definite function V is a function that satisfies $V(0) = 0$ and $V(x) > 0$ for $x \neq 0$

with the following change of variables: $Y^2 = V$, the upper bound on the derivative of the new Lyapunov function Y becomes linear and :

$$\dot{Y} \leq -\frac{\lambda_{\min}[Q]}{\lambda_{\max}[P]} Y + \frac{1}{2^{\frac{1}{2}} \lambda_{\min}^{\frac{1}{2}}[P]} \|P\gamma\|$$

after exponentially decaying transient, the solution x is globally uniformly ultimately bounded by

$$\|x\| \leq d = \left[\frac{\lambda_{\min}[Q]}{\lambda_{\max}[P]}\right]^{-1} \frac{1}{\lambda_{\min}[P]} \|P\gamma\|. \tag{4.10}$$

4.3.2 Vector Lyapunov Function

When the number of state increases, and hence the size of matrix P and Q, finding the solution to the system of linear equations for the elements of the matrix P that satisfies $PA + A^T P = -2Q$ becomes more complex. The work of Vector Lyapunov Function can be utilized to analyze the stability of a system based on several Lyapunov functions, where each function can satisfy less rigid requirements than in the classical Lyapunov's theorem.

Recall the system (4.6):

$$\dot{x} = f(t, x),$$

where x and $f(t, x)$ are n-dimensional vectors with $f(t, 0) = 0$. The stability of the equilibrium solution $x = 0$ can be analyzed via a vector Lyapunov function. Instead of analyzing the stability of system (4.6) by a single scalar Lyapunov function, a vector of Lyapunov-like functions $V \in C[R_+ \times R^n, R^N]$ with $N \leq n$ components, and the derivative-like function $D^+V(t, x)$ is defined as

$$D^+V(t, x) = \lim_{h \to 0^+} \sup \frac{1}{h} [V(t + h, x + hf(t, x)) - V(t, x)] \tag{4.11}$$

for $(t, x) \in [R_+ \times R^n]$. Each Lyapunov-like function here is assumed to be locally Lipschitz in x instead of continuous and differentiable $(V(t, x) \in C^1)$ as in Lyapunov stability analysis. The stability is analyzed through a comparison system:

$$\dot{U} = p(t, U),\ U(t_0) = U_0 \geq 0 \tag{4.12}$$

where $p \in C[R_+ \times R^n, R^N]$ and $p(t, U)$ is quasimonotone nondecreasing in U. With the assumption that

$$D^+V(t, x) \leq p(t, V(t, x)), \tag{4.13}$$

where the inequalities between vectors are componentwise and quasimonotonicity of $p(t,U)$ means that $U \leq R$, $U_i = R_i$ for $1 \leq i \leq N$ implies $p_i(t,U) \leq p_i(t,R)$. Then, the practical stability[5] of system (4.12) implies the corresponding practical stability properties of the system (4.6) with the following assumptions [22, page 33]:

(i) $p \in C[R_+ \times R^N, R^N], p(t,0) \equiv 0$ and $p(t,u)$ is quasimonotone nondecreasing in u for each $t \in R_+$

(ii) $V \in C[R_+ \times R^n, R_+^N]$, $V(t,x)$ is locally Lipschitz in x, and the function $V_0(t,x) = \Sigma_{i=1}^N V_i(t,x)$ is positive definite and decrescent.

(iii) $f \in C[R_+ \times S(\rho), R^n], f(t,0) \equiv 0$ and condition (4.13)

We consider here a linear comparison system

$$p(t,U(t,x)) = AU(t,x) + b \tag{4.14}$$

where the stability properties are given by the matrix $A = [a_{ij}]_{n\times n}$ and the vector $b = [b_{i1}]_{n\times 1}$. Then, $p(t,U) = AU + b$, with A Hurwitz and $b > 0$, is admissible to imply uniform strong ultimate bounded stability of system (4.6) [46].

4.3.3 Sliding Mode Control

A discrepancy of the actual plant and the mathematical model has driven the development of robust control methods. One particular approach of these methods is Sliding Mode Control [39, chapter 1].

A design of this controller can be summarized from an example in [39, chapter 1] as follows. For a system:

$$\begin{cases} \dot{x}_1 = x_2 & x_1(0) = x_{10}, \\ \dot{x}_2 = u + f(x_1, x_2, t) & x_2(0) = x_{20}, \end{cases} \tag{4.15}$$

where the states of the system $x_1 = x, x_2 = \dot{x}_1$ are position and velocity respectively, u is the control force and $f(x_1, x_2, t)$ is the disturbance that might comprise dry or viscous friction or other terms. The disturbance is assumed to be bounded from above by a known constant, e.g. $|f(x_1, x_2, t)| \leq L > 0$.

First, a sliding variable σ that is constituted by the systems states is defined

$$\sigma = \sigma(x_1, x_2) = x_2 + cx_1, \quad c > 0 \tag{4.16}$$

[5] Practical stability for a system means that there is an ultimate bound $|x(t)| < d$ of the solution of an ordinary differential equations initialized within another bound $|x_0| < a$. The same definition applies for a perturbed system by a non-vanishing but bounded perturbation $|g(t,x)| < \delta$.

This is a variable that would be driven to zero in finite time by the control $u(x_1, x_2)$. Note that as soon as $\sigma \equiv 0$ the system's dynamics becomes $\dot{x}_1 = -c\,x_1$ and x_1 vanishes to zero exponentially. Based on Lyapunov function, $V = \frac{1}{2}\sigma^2$, the feedback controller is designed. The derivative of this Lyapunov function is

$$\dot{V} = \sigma\dot{\sigma} = \sigma(cx_2 + f(x_1, x_2, t) + u) \tag{4.17}$$

with $u = -cx_2 + v$, Eq. 4.17 becomes

$$\dot{V} = \sigma(f(x_1, x_2, t) + v) = \sigma f(x_1, x_2, t) + \sigma v \leq |\sigma|L + \sigma v \tag{4.18}$$

with $v = -\rho\text{sign}(\sigma)$ where

$$\text{sign}(x) = \begin{cases} 1 & ,\text{x} > 0 \\ -1 & ,\text{x} < 0 \end{cases} \tag{4.19}$$

and

$$\text{sign}(0) \in [-1, 1] \tag{4.20}$$

with $\rho > L$,

$$\dot{V} \leq |\sigma|L - |\sigma|\rho = -|\sigma|(\rho - L). \tag{4.21}$$

Taking into account the inequality above for the derivative of Lyapunov function we conclude that σ converge to zero in finite time since $V = \sigma^2/2 \geq 0$ and

$$\dot{V} \leq -\alpha V^{1/2} = -\frac{\alpha}{\sqrt{2}}|\sigma|, \quad \alpha > 0 \tag{4.22}$$

Comparing Eq. 4.21 and Eq. 4.22

$$\dot{V} \leq -|\sigma|(\rho - L) = -\frac{\alpha}{\sqrt{2}}|\sigma| \tag{4.23}$$

then the control gain ρ is computed as

$$\rho = L + \frac{\alpha}{\sqrt{2}} \tag{4.24}$$

and u becomes

$$u = -cx_2 - \rho\text{sign}(\sigma). \tag{4.25}$$

From the initial conditions x_{10}, x_{20}, this controller will drive the sliding variable to zero $\sigma = 0$ in finite time, which is called reaching phase. Once the sliding variable is zero (sliding mode), it will remain zero with the same controller and the system dynamics is reduced into $\dot{x}_1 + cx_1 = 0$, which is called the sliding surface.

However, in practice, a zigzag motion is observed in the sliding mode due to the limited switching frequency, which is called chattering. One solution to attenuate chattering is to approximate the sign function with a sigmoid function:

$$\text{sign}(\sigma) \approx \frac{\sigma}{|\sigma| + \epsilon} \tag{4.26}$$

Under this smooth control law, the sliding variable will converge to a vicinity of the origin. This condition is called quasi-sliding mode, which has been used during this study.

5 Payload Estimation

This task is to estimate the mass in the mounted implement. In particular, we focus on the mass in an attached bucket. The commercially used state-of-the-art of most payload estimation algorithms that are based on linear interpolation work fine only when the estimation conditions are fairly close to the ones during calibration [3]. In this work, we investigate a payload estimation algorithm based on the equations of motion to improve the accuracy within varying estimation conditions, specifically the variation in bucket angle and lifting velocity, with the target accuracy of 2% Full Scale (FS) error. Moreover, this target is preferably achieved during regular operations.

As a robotics system, the mechanical equations of motion govern the FELs motions. The dynamic parameters involved in these expressions are commonly identified to improve the torque response for control purpose, rather than improving the identified parameters [48]. Within industrial robotics, the identification experiments are normally carried out with a carefully planned exciting trajectories. However, payload estimation in FELs is expected to be carried out in parallel to driver's normal operation, which is a monotonous lifting or lowering. For this reason, it is expected that smaller number of kinematic and dynamic parameters can be identified. However, within the particular application, some relatively good parameters can be extracted from the manufacturer's CAD model. Besides, a calibration procedure, as a current industry standard, can be used to estimate the discrepancies between CAD model and the physical system. With the limited number of parameters that can be estimated, obtaining a payload estimation within the desired accuracy becomes a problem to find the substantial model that can describe the FEL motions.

As the gravitational torque contributes the most to the total torque except for the fastest motion [26], it becomes the base of the proposed payload estimation algorithm. The

simplified quasi-static equations of motion of the loader becomes:

$$\begin{aligned} G_1(\boldsymbol{\theta}) &= g\overline{FM}s_1M_2 + gs_{12}M_2\overline{MX}_2 + gc_{12}M_2\overline{MY}_2 \\ &\quad + gc_1M_1\overline{MY}_1 + gs_1M_1\overline{MX}_1. \end{aligned} \tag{5.1}$$

The regressor and parameters to be identified are constructed depending on the considered assumptions of the real system, e.g. assuming the model and parameters from the CAD exactly represent the real system, M_2 will be the only unknown, which can be directly computed. However, several uncertainties are present in the real system, including, but not limited to, additional boom weights from hoses and fluid ($M_1 + \Delta M_1$) and an error in the location of the COG of link 2 ($\overline{MX}_2 + \Delta\overline{MX}_2, \overline{MY}_2 + \Delta\overline{MY}_2$) for different payload locations in the bucket. Moreover, varying boom COG is expected due to the varying boom sructure for different lift cylinder extensions ($\overline{MX}_1(x_1), \overline{MY}_1(x_1)$).

When all the uncertainties are considered, the regressor and parameters for a particular i-th set of measured joint angles becomes

$$G_1(i) = \phi(i)^T\theta^0 = \begin{bmatrix} g\overline{FM}s_1(i) \\ gs_{12}(i) \\ gc_{12}(i) \\ gs_1(i) \\ gc_1(i) \end{bmatrix}^T \begin{bmatrix} M_2 \\ M_2\overline{MX}_2 \\ M_2\overline{MY}_2 \\ M_1\overline{MX}_1 \\ M_1\overline{MY}_1 \end{bmatrix}. \tag{5.2}$$

Then, the parameters are estimated off-line using Matlab optimization Toolbox™ such that the focus of the work is about modeling instead of identification tools[1]. A set of experiments varying the estimation conditions, specifically lifting velocities and bucket angles, have been done to examine the accuracy and repeatability of possible estimation algorithms.

A reasonably accurate payload estimation is obtained when the boom COGs are calibrated first assuming that the bucket COGs are correct. Though these parameters are estimated as constants instead of functions, the payload estimation accuracy with this proposal lies within 5% FS error, which is reported in Paper C. It is also observed that the proposed estimation algorithm is less sensitive to variation in bucket angle since this parameter explicitly appears in the model.

[1] Another identification tool, namely algebraic method [40], has been investigated in simulation for a simple mechanical system. However, the work on model improvement has been carried on to achieve a 2% FS error instead of the work on identification method and this decision has stopped us from working further on algebraic method for payload estimation or investigating other identification methods.

As the calibration of boom COGs can not fulfill the desired accuracy of 2% FS error, several possible modifications have been investigated. It turns out that adding a pressure-based friction term, inspired by [9], in the equations of motion improves the acuracy to the desired level, which is reported in Paper D. Moreover, an on-line payload estimation has been performed with a similar attained accuracy.

The approach of estimating payload based on equations of motion is actually twofolds. A better estimation accuracy indicates a better model of the loader. Though the presented works have been investigated only with a bucket as implement and on a particular loader sample, but industry-standard, the same procedure is believed to work with different implements and different 2-DOF loaders with a straightforward modifications of the parameters.

6 Supportive Works

6.1 Hardware and Related Issues

Throughout this study, several hardware related investigations have been done. A brief summary of each activity is reported here.

6.1.1 Real Time Platform Comparison

This task was carried out to see the possibility to replace dSpace as a real time prototyping platform keeping the possibility to design and to tune controllers on-the-fly using the code developed in Matlab/Simulink. A comparison between dSpace DS1401 and MATLAB xPC target version 5.4 has been carried out and summarized in table 6.1.

Table 6.1: Comparison of dSpace DS 1401 and xPC Target v5.4 as a real-time prototyping platform.

Desirable feature	**DS 1401**	**xPC**
Online parameter modification	V	V
Data logging with labelled signal	V	V
Host signal monitoring	V	V[a]
I/O port flexibility	V[b]	X[c]
Memory direct access	V	V

[a] limited.
[b] time consuming.
[c] restricted to the initial plan

Several features are found similar in dSpace and xPC Target: the possibility to change parameters, e.g. constant gain, when the real-time target is running; the structured la-

bels for data logging; and the possibility to directly read/write the memory when e.g. a collaboration with external applications is required.

Meanwhile, there are also significant differences. The signal monitoring at the host PC in dSpace seems to have the same priority with other tasks whereas lower priority is observed in xPC Target. Besides, it is rather flexible to add hardwares in dSpace, even with the expected time-consuming process for cabling, whereas a careful initial plan of the possible connected hardwares is important in xPC Target.

6.1.2 IMU sensor connection

This task was carried out to change the IMU indirect connection available at the beginning of the thesis work, which provided the measurement through a driver in a desktop, to a direct connection to dSpace. The indirect connection shows noisier measurement than the direct one (Fig. 6.1) since the process in desktop is not performed in real time. As the final application must be done in real time, the controllers have been investigated based on the measurement with the IMU direct connection before a different sensor is selected to be used in the research experimental setup.

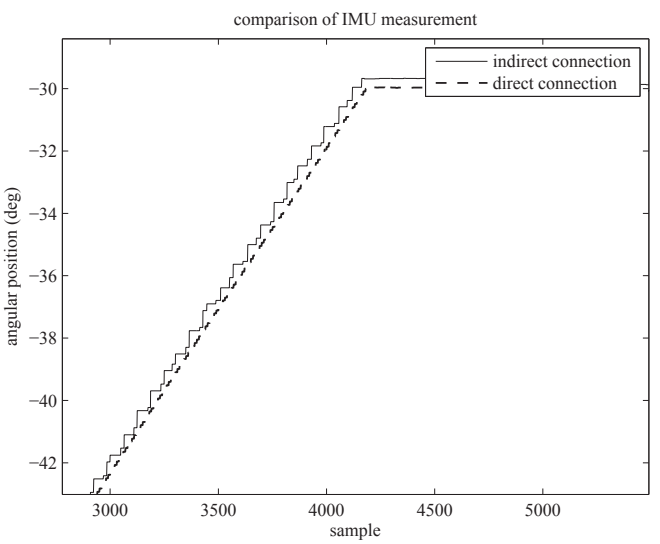

Fig. 6.1: Comparison of direct and indirect IMU measurements

A brief description of the direct connection is presented in the following. An RS232 connection has been built and the serial block from dSpace is utilized to decode the re-

ceived RS232 packets and output the message, message length, and the receiving status. Then, a driver have been developed based on the IMU message protocol [47] (Fig. 6.2). The finite state machine diagram in Fig. 6.3 is utilized in the reader. With this reader,

PREAMBLE	BID	MID	LEN	DATA	CHECKSUM

Fig. 6.2: IMU low level communication protocol. Preamble = Indicator of the start of a packet. BID = Bus Identifier. MID = Message Identifier. LEN = Message Length.

about 56 times of one lost message each was detected during one hour, which is still considered as a reasonable reader.

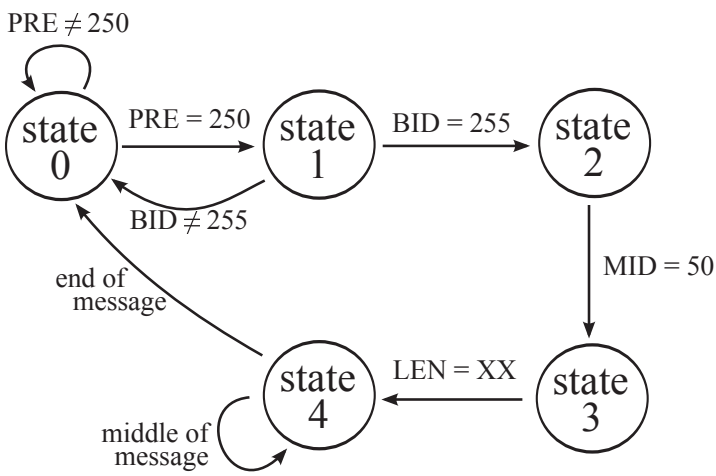

Fig. 6.3: A Finite State Machine design of the IMU reader. The length of the message (LEN) depends on the IMU configuration

6.1.3 Sensors Calibration

To compare different angular position sensors that are mounted on the research experimental setup, a calibration is required such that each sensor reading is based on the same assigned frames. The calibration implies finding the angular position offset θ_{ioff} for the rotational sensors

$$\theta_i = \theta_{ir} + \theta_{ioff}$$

and affine equation parameters for the linear sensors a_i, b_i in

$$x_i = a_i x_{ir} + b_i$$

where θ_{ir} denotes angular sensor output read in dSpace, x_{ir} denotes the cylinder extension value read in dSpace, x_i denotes the physical cylinder extension, θ_i denotes the physcial angular position and $i = 1, 2$ denotes the lift and tilt cylinder respectively.

Here, a calibration method is proposed when the sensors are already installed. Instead of uninstalling the sensors and tuning the offsets and parameters manually, the proposed method is processing the data from both linear and rotational sensors that are recorded from a manually performed motion that covers the whole joint space. With this data, the following optimization is proposed to obtain the θ_{ioff}, a_i, and b_i.

$$\begin{aligned} &\underset{\theta_{1off}}{\text{minimize}} \quad \sum_{r=1}^{N}(h_i^{-1}(\theta_{ir} - \theta_{ioff}) - (a_i^* \times x_{ir} + b_i^*))^2 \\ &\text{subject to} \quad (a_i^*,\, b_i^*) = \underset{a_i, b_i}{\arg\min} \quad \sum_{r=1}^{N}(h_i^{-1}(\theta_{ir} - \theta_{ioff}) - (a_i \times x_{1r} + b_i))^2. \end{aligned} \tag{6.1}$$

The minimizer of linear equation parameters are obtained using Least Square given an angular offset from another optimization process and the minimizer of angular offset is obtained using MATLAB Optimization toolbox. The cost function of both optimizations is the square of cylinder extension error between the one computed using the geometric transformation from the angular position reading, given the required geometric parameters, and the one computed from the cylinder extension reading.

This idea has been applied to the tilt cylinder calibration (with $i = 2$) and compared to the manual calibration[1]. The obtained parameters from the proposed calibration are close to the ones from the manual calibration (Table 6.2). The maximum error in cylinder extension is around 2.5 mm (Fig. 6.4).

Table 6.2: Comparison of the manual and proposed calibration for tilt cylinder.

Parameter		Manual calibration	Proposed calibration
Offset θ_{2off} (degree)		-125.62	-126.68
Linear parameters	a_2	3.1781	3.1431
	b_2	-1.1987	-1.3296

Though the maximum error with the proposed calibration is rather small, it shows a dependency on the cylinder extension. This is because the assumptions made in the op-

[1]The manual calibration of linear sensor is done by uninstalling the sensors and comparing the physical cylinder extension and the sensor reading in dSpace. While the manual calibration of the angular position sensor is obtained from the transformed angular position of the tilt maximum extension assuming that the transformation is error-free.

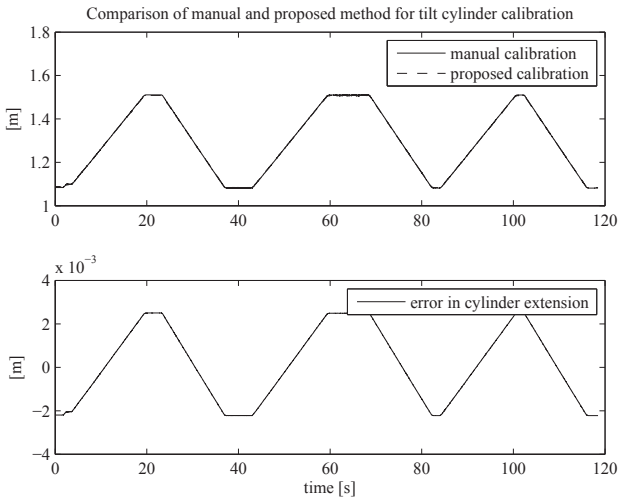

Fig. 6.4: Comparison of direct and indirect IMU measurements

timization does not take into account the possible discrepacy in the physical system. For example, the linearity asumption in the linear sensor does not take into account the possible tilted sensor installation. Bigger deviation is expected with more disregarded physical facts. Conversely, the proposed method might be useful to investigate the disregarded physical facts. Besides, depending on the desired accuracy, this method might be useful for sensor calibration when uninstalling sensors is not an option.

6.2 Differentiator

Throughout this work, a numerical differentiator is used to estimate the derivatives of various directly measured signals that are needed, e.g. the derivative of error in the proposed tuning procedure for the ESL controller and also to estimate cylinders' velocity in the proposed algorithm to handle flow limitation.

One of commonly used computational procedures to estimate derivatives is known as a high-gain-observer. An example of a standard high-gain observer for a second order system $\dot{x}_1 = x_2, \dot{x}_2 = f(x_1, x_2)$ with measurable x_1 and uncertain $f(\cdot)$ can be implemented as a solution of the following differential equations:

$$\dot{\hat{x}}_1 = -\frac{k_1}{\epsilon}e + \hat{x}_2 \tag{6.2}$$

$$\dot{\hat{x}}_2 = -\frac{k_2}{\epsilon^2}e + \delta(\cdot) \tag{6.3}$$

where $e = \hat{x}_1 - x_1$ and $\delta(\cdot)$ denotes a possible model of the uncertain function $f(\cdot)$. The introduced ϵ shows a clear advantage of reducing this value to attenuate the disturbance, defined by the difference between $\delta(\cdot)$ and $f(\cdot)$, in the error-dynamics representation with scaled estimation error [19, page. 613]. However, in the presence of measurement noise, ϵ should be chosen considering the trade-off between noise amplification and disturbance rejection, since reducing it leads to a higher amplitude of high-frequency component of estimation errors due to noise amplification.

When there is no model of the system and $\delta(\cdot)$ is taken to be 0, this second order high gain observer becomes a differentiator as it is estimating the derivative of the measured signal, i.e. $\dot{x}_1$ without any knowledge of a model generating signal. As a part of the controller we propose for ESL, we set ϵ to 1 and $k_2 = k_1^2/4$ to simplify the tuning procedure. The latter is based on a critically damped condition of a second order system. Thus, we have one parameter to tune the differentiator.

The same parametrization is done to obtain the differentiator parameters for estimating the cylinders velocity to test the proposed algorithm to cope with flow limitation. By trial and error, k_1 is chosen such that the estimation converges as fast as possible with a certain level of noise amplification. For this algorithm, k_1 and k_2 are equal to 9 and 20.25 respectively.

Besides High Gain Observer, velocity estimation based on Super Twisting [24] was also investigated:

$$\dot{\hat{x}}_1 = -1.5L^{1/2}|e|^{1/2}\text{sign}(e) + \hat{x}_2 \tag{6.4}$$

$$\dot{\hat{x}}_2 = -1.1L\text{sign}(e) \tag{6.5}$$

The tuning of this differentiator requires knowledge of an upper bound on the second derivative and is done by setting $L > |\bar{\ddot{x}}_1|$. Here, the maximum acceleration is 8 rad/s^2, obtained by differentiating the spline approximation[2] of a recorded position measurement.

A comparison to velocity estimation from an IMU sensor is shown in Fig. 6.5. Noisier estimation is observed in the constant velocity region (around 7 s) due to overcompensation. During this constant velocity region, the acceleration is around 0 rad/s^2 such that

[2]A MATLAB fitting function with smoothing spline option is used for this approximation, e.g. `fit(x,y,'smoothingspline','SmoothingParam', 0.9998);`

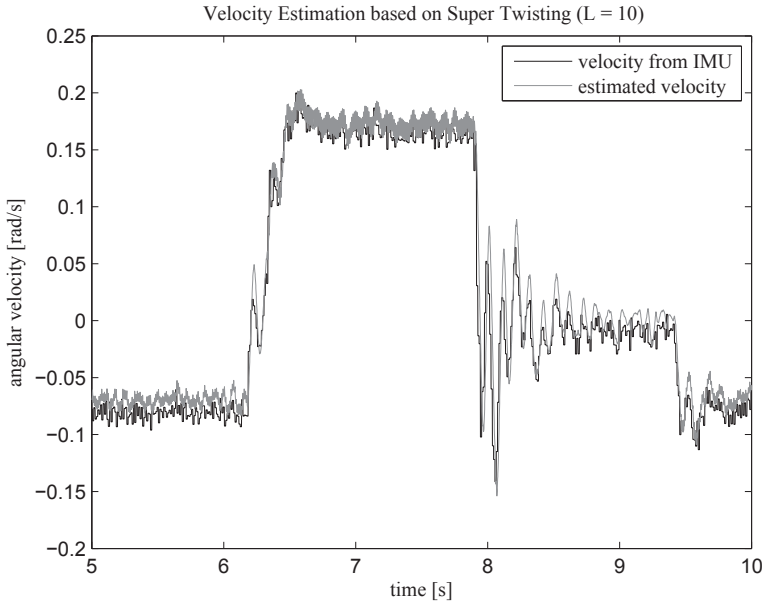

Fig. 6.5: Comparison of velocity estimation using Super Twisting algorithm and velocity information from IMU sensor

a constant $L = 10$ becomes too large contributing to amplification of the measurement noise in a similar way as with high-gain observers. However, further possible works, e.g. ST with varying gain, were not pursued.

7 Summary of Contributions

Paper A: Automation of Front End Loaders: Self Leveling Task In this paper, it is observed that different controllers are required for lifting and lowering motions to realize ESL task within a certain accuracy due to the impact of the gravity. A linear controller is enough to maintain the bucket position in lifting motion whereas an additional perturbation rejection term is required in the lowering motion to satisfy a certain tracking error. Moreover, the combination of Active Disturbance Rejection Control and Sliding Mode Control to deal with perturbation results in a good performance in terms of sufficiently low steady state error and oscillations. All the controller parameters in this paper are tuned by trial and error.

Paper B: Control and Tuning Procedure of a Cylinder in Mobile Hydraulics In this paper, a tuning procedure based on a quadratic vector Lyapunov function is proposed to obtain the controller parameters for lowering motions, that are constituted by the proportional controller, disturbance observer and relay controller, to achieve a steady-state error in maintaining the self-leveling within the required 2 degrees. A comparison between the tuned controller and PI controller shows that the proposed controller is less sensitive to lowering velocities.

Paper C: Payload Estimation in Front-End Loaders In this paper, the challenges of payload estimation in FELs are presented. An off-line estimation procedure based on simplified quasi-static equations of motion that starts with the calibration of boom center of gravity before estimating the payload is proposed. This proposal results in the estimation accuracy of 5% Full Scale error, which is evaluated within a set of experiments with the variation of operating velocities and bucket angles. The experiments are performed on a research experimental set-up that consists of an industry-standard loader, a stationary tractor, and a dSpace-based prototyping system.

Paper D: Improvement of Model-Based Payload Estimation for Agricultural Front-End Loaders In this paper, a pressure-based friction model is added to the simplified equations of motion, which have been used in Paper C, to have a more accurate model of FELs to obtain a more accurate payload estimation. The offline payload estimation, based on the estimated friction parameters in the proposed calibration step, results in an accuracy of 2% FS error in a set of experiments with the variation of the operating velocity and bucket angle. Moreover, an on-line estimation has also been investigated for the payload estimation step while keeping the offline estimation of friction parameters during the calibration phase.

8 Conclusions and Future Work

8.1 Conclusions

In this thesis, driven by the trend towards automation in agriculture and a demand initiated within Ålö AB, one of the leading producers of front-end loaders, we have performed a development and an evaluation of proposed solutions for both Electronic Self Leveling (ESL) and payload estimation tasks, with a particular hydraulic valve with inlet pressure compensator. Our results indicate the feasibility of sensor-based automation for Front-End Loaders. Particularly, model-based solutions are proposed to realize the tasks and experimentally tested on an up-to-date industry-standard equipment enhanced by a standard professional fast control prototyping system, an integrated hardware and software bundle, in laboratory conditions.

For the Electronic Self Leveling task, a model of a hydraulic cylinder is utilized for analysis and control design. A controller that is constituted by a commonly used linear controller, a disturbance estimation term, a relay controller and a dead-zone compensation is proposed and tuned to achieve a steady-state error below 2 degrees in lowering motions, according to the specifications posed by the company. The proposed controller is less sensitive to lowering velocity in comparison to a standard proportional-integral controller.

Moreover, the proposed fault mitigation, based on the ESL requirement from mechanical viewpoint, is able to cope with the flow supply limitation. This has a high industrial importance, and for Ålö in particular. As the FELs are intended to work without any information from different possible tractors, such as the actual engine RPM setting and perhaps also the hydraulic pump operating output, being able to detect saturation and deal with insufficient flow becomes very important.

For payload estimation task, simplified mechanical equations of motion are improved by incorporating a pressure based friction model to represent the loader's quasi-static motions and hence improving the payload estimation in the constant velocity region of lifting motion. Based on the estimated friction parameters in calibration step, the payload estimation accuracy reaches 2% FS error in a set of experimental data with variation in bucket angles and lifting velocities.

8.2 Future Work

In this work, the solution to perform ESL task has been proposed and investigated for the steady-state region in lowering motions. Possible immediate directions for future works are the following:

- Improving transient behavior with minimized or automated tuning of parameters. A brief investigation on adding a feed forward term shows an improvement in transient region with unclear tuning procedure that can be pursued further.
- Improving lifting motion performance. Though a linear controller is enough to realize ESL at a certain flow supply level, load dependency is observed in tilt-out motion with the particular valve under consideration, which is the required correction in lifting motion. Further observation is needed to evaluate the linear controller and to propose a systematic procedure to tune its parameters to satisfy the desired 2 degrees tracking error.
- Investigation of solutions in varying ambient temperatures. The model used for control design and analysis to realize ESL in this work considers a turbulent flow across the orifice. This model covers most of the working conditions of the system, except the extremely cold temperature where a laminar flow possibly occurs. As temperature decreases, the oil viscosity increases and hence the Reynolds number decreases.
- Investigating hydraulics-redesign-based solutions. The proposed solution in this thesis is mainly from control systems perspective. It is also interesting to investigate possible solutions from hydraulics perspective, e.g. different valve or pump configurations or different components in the hydraulic circuit, to investigate automation for this system.

For payload estimation task, several possible future works are:

- Estimation in lowering motion. The proposed estimation algorithm neglects the inertia and Coriolis terms in the equations of motion. Though the impact velocity is present in the pressure based friction, it is interesting to investigate how the algorithm performs in lowering motions, which are much faster than lifting motions.
- Estimation on uneven ground. It is interesting to investigate the impact of the estimation on an uneven ground, including the possible additional sensors that are required for this estimation condition.

Another possible future work is from FEL modeling. Part of this thesis work has been allocated to model the Front-End Loader for simulation, that consists of a mechanical part, a hydraulics part and a transformation that links both parts. In the hydraulic modeling, it is not clear how to introduce the pressure head, the pressure difference due to different vertical position, into the generated hydraulic force as the cylinder motion is always affected by the gravity.

Having mentioned more challenges, investigations and possible works that can be done in the future, the work presented here still requires more evaluation to be transfered to the product development process. Moreover, all the presented evaluation has been carried out under operating conditions that are sufficient to prove the concept of the proposed solutions in laboratory. Further extensive evaluation in field, employing an industry-standard embedded system and taking into account additional disturbances, is required to verify their usability as products to assist farmers with more automatic features. However, the project has been good for both university and company. Several challenges from industry are identified and theoretical-based modeling and solutions are introduced from academia to drive more fruitful research collaboration.

Bibliography

Bibliography

[1] AFEB. Eu farms and farmers in 2013: an update. http://ec.europa.eu/agriculture/sites/agriculture/files/rural-area-economics/briefs/pdf/009_en.pdf, 2015.

[2] S. Aranovskiy. Report on hydraulics models. Technical report, Umeå University, January 2014.

[3] N. Bennet, A. Walawalkar, and C. Schindler. Payload estimation in excavators: Model based evaluation of current payload estimation system. In *Proceeding of 3rd Commercial Vehicle Technology Symposium*, volume 3, 2014.

[4] M. Berducat. Agricultural robotics (in open fields. http://www.eurageng.eu/sites/eurageng.eu/files/ageng_papers/SIMA%20Paris%202015/Agricultural%20Robotics%20Berducat.pdf, 2015.

[5] J. Billingsley, A. Visala, and M. Dunn. *Robotics in Agriculture and Forestry*, pages 1065–1077. Springer Berlin Heidelberg, Berlin, Heidelberg, 2008.

[6] B. S. Blackmore, B. S. Stour, W. Wang, and B. Runov. Robotic agriculture - the future of agricultural mechanisation? In *5th European Conference on Precision Agriculture. ed. J. Stafford, V.*, pages 621–628, 2005.

[7] J. E. Bobrow and K. Lum. Adaptive, high bandwidth control of a hydraulic actuator. In *Proceedings of the 1995 American Control Conference,*, volume 1, pages 71–75 vol.1, Jun 1995.

[8] A. Bonchis, P. Corke, and D. Rye. Experimental evaluation of position control methods for hydraulic systems. *IEEE Transactions on Control Systems Technology*, 10(6):876–882, 2002.

[9] A. Bonchis, P. I. Corke, and D. C. Rye. A pressure-based, velocity independent, friction model for asymmetric hydraulic cylinders. In *Proceedings 1999 IEEE International Conference on Robotics and Automation*, volume 3, pages 1746–1751, 1999.

[10] COA. Preliminary report highlights. u.s. farm and farmers. https://www.agcensus.usda.gov/Publications/2012/Preliminary_Report/Highlights.pdf, 2014.

[11] S. Dadhich, U. Bodin, and U. Andersson. Key challenges in automation of earth-moving machines. *Automation in Construction*, 68:212 – 222, 2016.

[12] John Deere. Row crop tractor loaders. https://www.deere.com/en_US/products/equipment/front-end-loaders/row-crop-tractor-loaders/row-crop-tractor-loaders.page, 2017.

[13] L. Emmi, M. Gonzalez de Soto, G. Pajares, and P. Gonzalez de Santos. New trends in robotics for agriculture: Integration and assesment of a real fleet of robots. *The Scientific World Journal*, 2014(404059):1–21, 2014.

[14] L. Ericson. Valve Controlled Systems. https://www.iei.liu.se/flumes/tmhp02/filarkiv/exchangestud/lectures/1.546382/Lecture8_Valve_controlled_systems.pdf, February 2014.

[15] P. M. Granitto, P. F. Verdes, and H. A. Ceccatto. Large-scale investigation of weed seed identification by machine vision. *Computers and Electronics in Agriculture*, 47(1):15 – 24, 2005.

[16] P. La Hera, U. Mettin, I. R. Manchester, and A. Shiriaev. Identification and control of a hydraulic forestry crane. *{IFAC} Proceedings Volumes*, 41(2):2306 – 2311, 2008.

[17] P. M. La Hera and D. Ortiz Morales. Modeling dynamics of an electro-hydraulic servo actuated manipulator: A case study of a forestry forwarder crane. In *World Automation Congress 2012*, pages 1–6, June 2012.

[18] J. Johnson. Understanding parallel connected valves. http://hydraulicspneumatics.com/200/TechZone/SystemInstrumen/Article/False/84693/TechZone-SystemInstrumen, 2009.

[19] H.K. Khalil. *Nonlinear Systems*. Pearson Education. Prentice Hall, 2002.

[20] W. Khalil and E. Dombre. *Modeling, Identification and Control of Robots*. Jordan Hill, GB: Butterworth-Heinemann., 2004. Retrieved from http://www.ebrary.com.

[21] J. Koivumäki and J. Mattila. The automation of multi degree of freedom hydraulic crane by using virtual decomposition control. In *2013 IEEE/ASME International Conference on Advanced Intelligent Mechatronics*, pages 912–919, July 2013.

[22] V. Lakshmikantham, V.M. Matrosov, and S. Sivasundaram. *Vector Lyapunov Functions and Stability Analysis of Nonlinear Systems*. Mathematics and Its Applications. Springer Netherlands, 1991.

[23] J. I. Latorre-Biel, I. Arana, T. Ballesteros, J. M. Pintor, and J. R. Alfaro. Front end loader with automatic levelling for farm tractors. *Biosystems Engineering*, 148:111 – 126, 2016.

[24] A. Levant. Robust exact differentiation via sliding mode technique. *Automatica*, 34(3):379 – 384, 1998.

[25] A. Levant. Higher order sliding modes and arbitrary-order exact robust differentiation. In *Proceedings of 2001 European Control Conference*, pages 996–1001, Sept 2001.

[26] D. Ma and J. M. Hollerbach. Identifying mass parameters for gravity compensation and automatic torque sensor calibration. In *Proceedings of IEEE International Conference on Robotics and Automation*, volume 1, pages 661–666, Apr 1996.

[27] J. Mattila, J. Koivumaki, D. Caldwell, and C. Semini. A survey on control of hydraulic robotic manipulators with projection to future trends. *IEEE/ASME Transactions on Mechatronics*, PP(99):1–1, 2017.

[28] H.E. Merritt. *Hydraulic Control Systems*. Wiley, New York, 1976.

[29] D. O. Morales, P. La Hera, U. Mettin, L. B. Freidovich, A. S. Shiriaev, and S. Westerberg. Steps in trajectory planning and controller design for a hydraulically driven crane with limited sensing. In *2010 IEEE/RSJ International Conference on Intelligent Robots and Systems*, pages 3836–3841, Oct 2010.

[30] D. O. Morales, S. Westerberg, P. La Hera, U. Mettin, L. B. Freidovich, and A. S. Shiriaev. Open-loop control experiments on driver assistance for crane forestry machines. In *2011 IEEE International Conference on Robotics and Automation*, pages 1797–1802, May 2011.

[31] D. O. Morales, S. Westerberg, P. X. La Hera, U. Mettin, L. Freidovich, and A. Shiriaev. Increasing the level of automation in the forestry logging process with crane trajectory planning and control. *Journal of Field Robotics*, 31(3):343–363, 2014.

[32] S. C. Mukhopadhyay, G. S. Gupta, and J. W. Howarth. Embedded microcontroller and sensors based front end loader control system. In *2008 IEEE Instrumentation and Measurement Technology Conference*, pages 1509–1514, May 2008.

[33] R. Murray. System modeling. online, October 2004.

[34] S.Y. Najafi. *Automatic Control of A Front-End Loader with Applications to Bucket Self-Leveling*. Umeå University [M.Sc. thesis], Umeå, Sweden, 2012.

[35] N. Niksefat and N. Sepehri. Designing robust force control of hydraulic actuators despite system and environmental uncertainties. *IEEE Control Systems Magazines*, 21(2):66–77, Apr 2001.

[36] T. Pilarski, M. Happold, H. Pangels, M. Ollis, K. Fitzpatrick, and A. Stentz. The demeter system for automated harvesting. *Autonomous Robots*, 13(1):9–20, 2002.

[37] L. J. Puglisi, R. J. Saltaren, C. Garcia, and I. A. Banfield. Robustness analysis of a {PI} controller for a hydraulic actuator. *Control Engineering Practice*, 43:94 – 108, 2015.

[38] N. Sepehri. *Dynamic Simulation and Control of Teleoperated Heavy-Duty Hydraulic Manipulators*. PhD Thesis, University of British Columbia, Vancouver, October 1990.

[39] Y. Shtessel, C. Edwards, L. Fridman, and A. Levant. *Sliding mode control and observation*. Springer, 2014.

[40] H. Sira-Ramírez, C. G. Rodríguez, J. C. Romero, and A. L. Juárez. *Algebraic Identification and Estimation Methods in Feedback Control Systems*. Wiley Publishing, 1st edition, 2014.

[41] G. A. Sohl and J. E. Bobrow. Experiments and simulations on the nonlinear control of a hydraulic servosystem. *IEEE Transactions on Control Systems Technology*, 7(2):238–247, Mar 1999.

[42] A. Stentz, J. Bares, S. Singh, and P. Rowe. A robotic excavator for autonomous truck loading. In *Proceedings. 1998 IEEE/RSJ International Conference on Intelligent Robots and Systems. Innovations in Theory, Practice and Applications (Cat. No.98CH36190)*, volume 3, pages 1885–1893 vol.3, Oct 1998.

[43] G. Tao and P.V. Kokotovic. Adaptive control of plants with unknown dead-zones. *IEEE Transactions on Automatic Control*, 39(1):59–68, Jan 1994.

[44] V. I. Utkin and A. S. Poznyak. Adaptive sliding mode control with application to super-twist algorithm: Equivalent control method. *Automatica*, 49(1):39 – 47, 2013.

[45] C. Vázquez, S. Aranovskiy, and L. Freidovich. Sliding mode control of a forestry-standard mobile hydraulic system. In *Proceeding of 2014 13th International Workshop on Variable Structure Systems (VSS)*, pages 1–6, June 2014.

[46] C. Vázquez, J. Collado, and L. Fridman. Control of a parametrically excited crane: A vector lyapunov approach. *IEEE Transactions on Control Systems Technology*, 21(6):2332–2340, Nov 2013.

[47] Xsens. *MT Low-Level Communication Protocol Documentation*, 2009.

[48] Y. H. Zweiri. Identification schemes for unmanned excavator arm parameters. *International Journal of Automation and Computing*, 5(2):185–192, 2008.